

Supporting Information for:

# Improving the Folding of Supramolecular Copolymers by Controlling the Assembly Pathway Complexity

Gijs M. ter Huurne,<sup>†</sup> Lafayette N. J. de Windt,<sup>†</sup> Yiliu Liu,<sup>†</sup> E. W. Meijer,<sup>†</sup> Ilja K. Voets<sup>\*,†</sup> and Anja R. A. Palmans<sup>\*,†</sup>

<sup>†</sup>Institute for Complex Molecular Systems, Laboratory of Macromolecular and Organic Chemistry, Eindhoven University of Technology, P.O. Box 513, 5600 MB, Eindhoven, The Netherlands.

1. Instrumentation.....	2
2. Materials.....	2
3. Monomer, BTA-C <sub>11</sub> -NH <sub>2</sub> and polymer synthesis and characterization.....	3
Synthesis of pentafluorophenyl acrylate ( <b>3</b> ) .....	3
RAFT-polymerization of pentafluorophenyl acrylate ( <b>P1</b> ).....	5
Endgroup modification of poly(pentafluorophenyl acrylate) ( <b>P2</b> ) <sup>S1</sup> .....	6
Synthesis of 5-(methoxycarbonyl)isophthalic acid ( <b>6</b> ) .....	8
Synthesis of methyl 3,5-bis(chlorocarbonyl)benzoate ( <b>7</b> ) .....	10
Synthesis of ( <i>S,S</i> )-BDA monomethyl ester ( <b>9</b> ) .....	11
Synthesis of ( <i>S,S</i> )-BDA monoacid ( <b>10</b> ) .....	12
Synthesis of 1-Undecanol-11-phthalimide ( <b>13</b> ).....	13
Synthesis of 11-Amino-1-undecanol ( <b>14</b> ) .....	14
Synthesis of ( <i>S,S</i> )-BTA-C <sub>11</sub> -OH ( <b>15</b> ) .....	15
Synthesis of ( <i>S,S</i> )-BTA-C <sub>11</sub> -tosylate ( <b>16</b> ).....	17
Synthesis of ( <i>S,S</i> )-BTA-C <sub>11</sub> -N <sub>3</sub> ( <b>17</b> ).....	19
Synthesis of ( <i>S,S</i> )-BTA-C <sub>11</sub> -NH <sub>2</sub> ( <b>18</b> ) .....	20
General post-functionalization procedure ( <b>P0-0</b> , <b>P0-20</b> , <b>P5-15</b> , <b>P10-0</b> , <b>P10-10</b> , <b>P15-5</b> , <b>P20-0</b> ).....	22
4. Sample preparation procedure .....	24
5. Dynamic and static light scattering .....	25
6. Circular dichroism spectroscopy .....	28
7. Small-angle neutron scattering .....	30
8. References.....	33

## 1. Instrumentation

$^1\text{H}$ - and  $^{13}\text{C}$ -NMR spectra were recorded on a Varian 400MR 400 MHz or a Varian Mercury Vx 400 MHz (400 MHz for  $^1\text{H}$ -NMR and 100 MHz for  $^{13}\text{C}$ -NMR). The  $^1\text{H}$ -NMR chemical shifts ( $\delta$ ) are reported in ppm downfield from tetramethylsilane (TMS).  $^{13}\text{C}$ -NMR chemical shifts are reported downfield from TMS using the resonance of the deuterated solvent as internal standard. Abbreviations used are br = broad, d = doublet, dd = double doublet, m = multiplet, p = pentet, s = singlet, t = triplet and q = quartet.

Infrared spectroscopy was measured using a PerkinElmer FT-IR Spectrum Two equipped with a Perkin-Elmer UATR Two.

Matrix assisted laser desorption/ ionization time of flight mass spectra (MALDI-TOF-MS) was acquired using a Bruker Autoflex Speed MALDI-TOF using  $\alpha$ -cyano-4-hydroxycinnamic acid (CHCA) or *trans*-2-[3-(4-*tert*-butylphenyl)-2-methyl-2-propenylidene]malononitrile (DCTB) as matrices.

Size exclusion chromatography (SEC) measurements were performed on a Shimadzu Prominence-i LC-2030C 3D with a Shimadzu RID-20A refractive index detector. As elution, THF containing 10 mM LiBr (flow = 1 mL min<sup>-1</sup>) was used operating at 40 °C with a mixed-C and mixed-D column combined in series (exclusion limit = 2.000.000 g mol<sup>-1</sup>; 7.5 mm i.d. × 300 mm) calibrated with poly(styrene) (Polymer Laboratories).

DMF-SEC measurements were performed on a PL-GPC-50 plus from Polymer Laboratories (Varian Inc. Company) with a refractive index detector. As elution, dimethylformamide containing 10 mM LiBr (flow = 1 mL min<sup>-1</sup>) was used operating at 50 °C with a Shodex GPC-KD-804 column (exclusion limit = 400.000 Da; 0.8 cm i.d. × 300 mm) calibrated with poly(ethyleneoxide) (Polymer Laboratories).

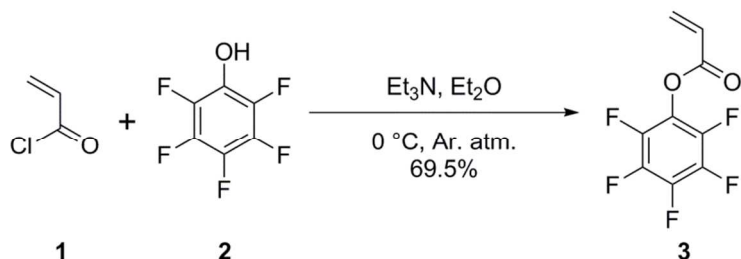
Density measurements were performed on an Anton Paar DMA 5000 M.

## 2. Materials

All commercial reagents were purchased from Aldrich and used as received unless stated otherwise. All solvents were purchased from Biosolve and the deuterated solvents were purchased from Cambridge Isotopes Laboratories. Dry solvents were obtained with an MBRAUN Solvent Purification System (MB-SPS). Jeffamine<sup>®</sup> M-1000 polyetheramine (**2**) was provided by Huntsman.

### 3. Monomer, BTA-C<sub>11</sub>-NH<sub>2</sub> and polymer synthesis and characterization

#### Synthesis of pentafluorophenyl acrylate (**3**)



Pentafluorophenol (**1**) (20.0 g, 109 mmol) and triethylamine (18 mL, 130 mmol) were dissolved in dry diethylether (200 mL). This solution was placed under an argon atmosphere and cooled using an ice bath. Acryloyl chloride (**2**) (11 mL, 135 mmol) was diluted with diethylether (100 mL) and slowly added to the reaction mixture using a dropping funnel. The reaction was allowed to reach room temperature while the conversion was monitored using <sup>19</sup>F-NMR spectroscopy. Upon reaching full conversion, the formed precipitate was removed via filtration and the solvent was evaporated. Product **3** was purified using column chromatography (silica, *n*-heptane) (17.95 g, 75 mmol, 69.5 %).

<sup>1</sup>H-NMR (400 MHz, CDCl<sub>3</sub>): δ 6.72 (dd, *J* = 17.3, 0.9 Hz, 1H), 6.37 (dd, *J* = 17.3, 10.5 Hz, 1H), 6.18 (dd, *J* = 10.6, 1.0 Hz, 1H).

<sup>13</sup>C-NMR (100 MHz, CDCl<sub>3</sub>): δ 161.8, 142.7, 141.0, 140.2, 139.4, 138.5, 136.9, 135.4, 125.5.

<sup>19</sup>F-NMR (376 MHz, CDCl<sub>3</sub>): δ -152.2 - -153.2 (m), -158.0 (t, *J* = 21.7 Hz), -162.0 - -163.0 (m).

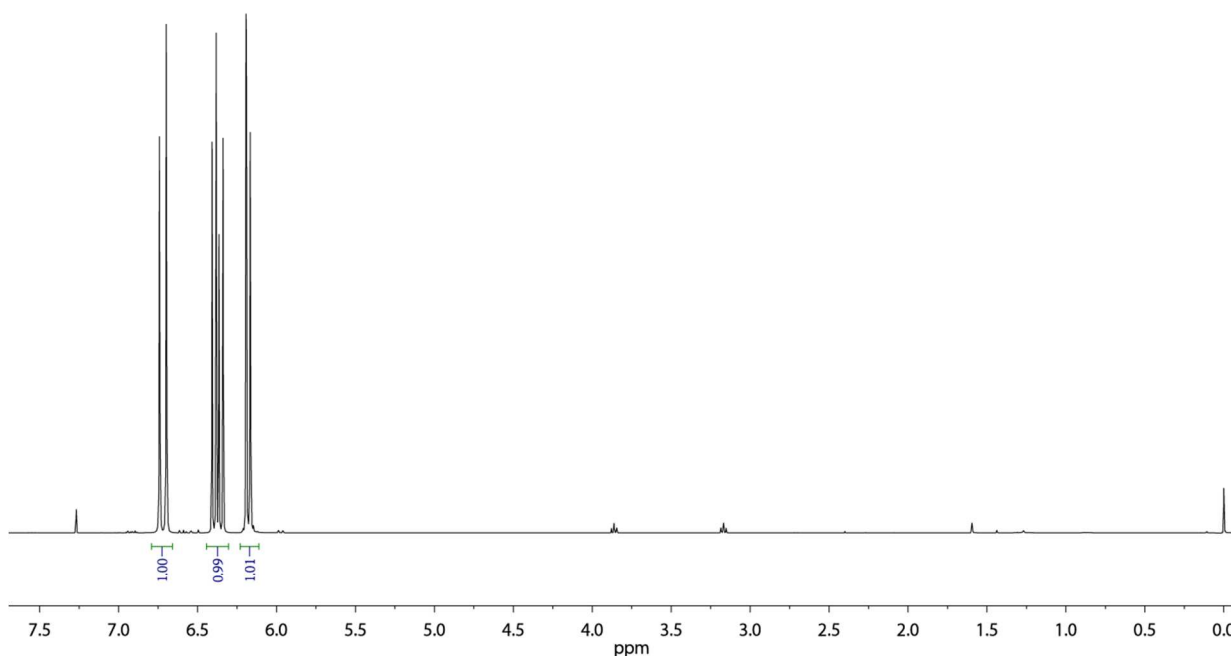


**Figure S1:** The <sup>1</sup>H-NMR spectrum of pentafluorophenyl acrylate monomer **3** in CDCl<sub>3</sub>.

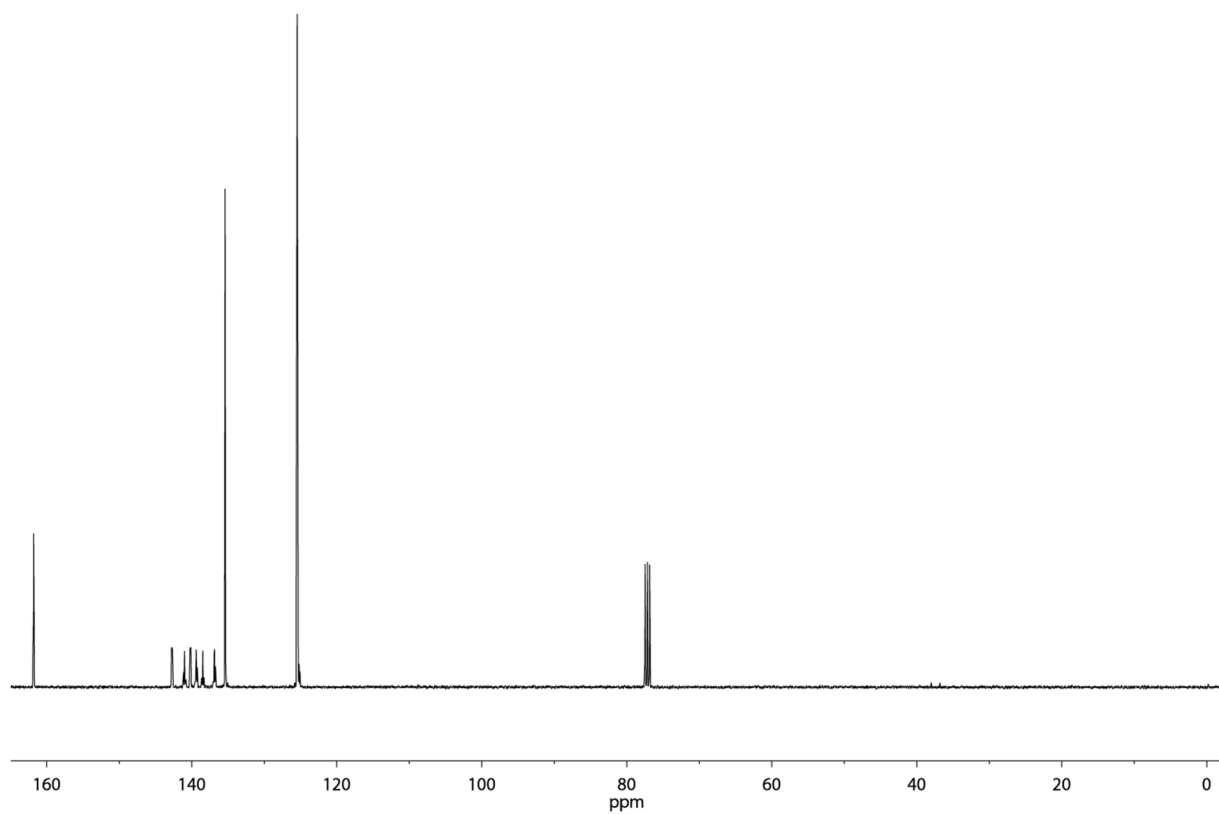


**Figure S2:** The  $^{13}\text{C}$ -NMR spectrum of pentafluorophenyl acrylate monomer **3** in  $\text{CDCl}_3$ .

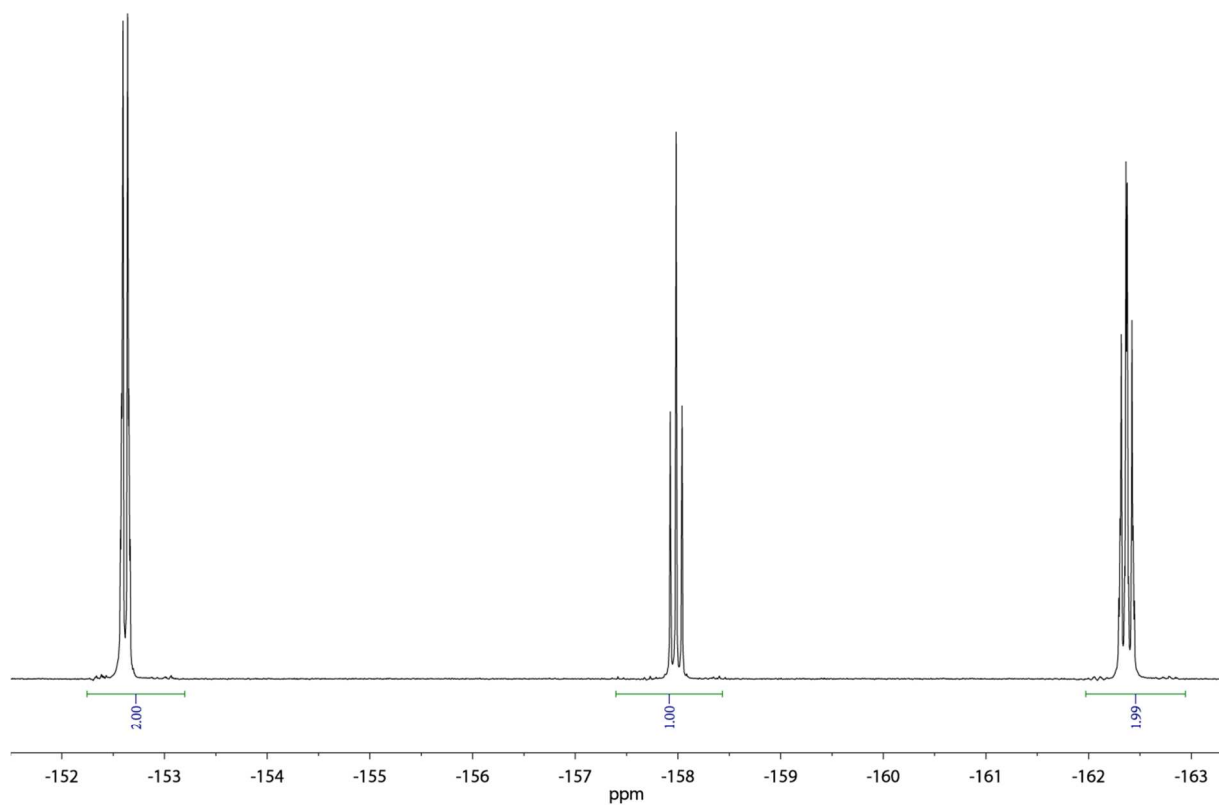
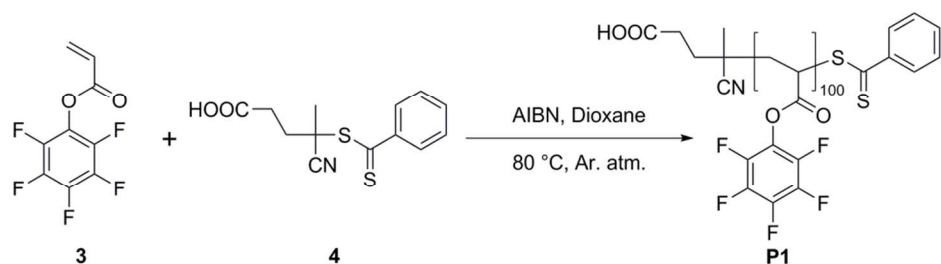


**Figure S3:** The  $^{19}\text{F}$ -NMR spectrum of pentafluorophenyl acrylate monomer **3** in  $\text{CDCl}_3$ .

### RAFT-polymerization of pentafluorophenyl acrylate (P1)



Pentafluorophenyl acrylate (**3**) (10.23 g, 43.0 mmol), 2,2'-azobis(2-methylpropionitrile) (AIBN) (7.04 mg, 0.04 mmol) and 4-cyano-4-(phenylcarbonothioylthio)pentanoic acid (**4**) (80.1 mg, 0.29 mmol) were dissolved in anhydrous dioxane (10 mL). The mixture was degassed by bubbling argon for one hour. The polymerization was started by placing the Schlenk tube in a preheated oil bath at 80 °C. After  $\pm 120$  minutes the polymerization was quenched by placing the reaction vessel in a liquid nitrogen bath. Using  $^{19}\text{F}$ -NMR spectroscopy, the final conversion of the polymerization was determined to be 66%. Based on this conversion the average degree of polymerization was determined to be 100. All solvent was removed using vacuum. The polymer was redissolved in a small amount of DCM and purified via precipitation in cold *n*-pentane (3 $\times$ ). Polymer **P1** was obtained as a bright pink solid (6.73 g).

$^{19}\text{F}$ -NMR (376 MHz,  $\text{CDCl}_3$ ):  $\delta$  -153.3 (br), -156.7 (br), -162.2 (br).

SEC (THF):  $M_n = 12.5 \text{ kg mol}^{-1}$ ,  $D_M = 1.27$ .

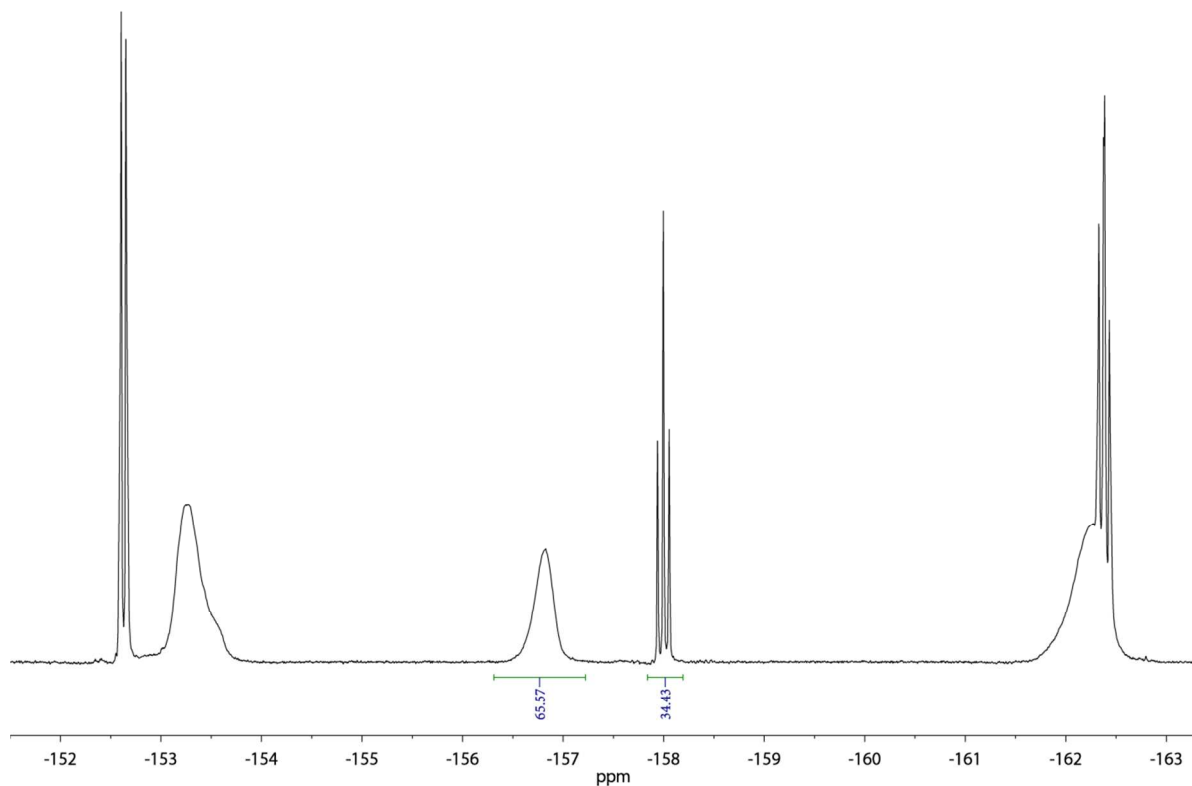


**Figure S4:** The final conversion of the polymerization as determined via  $^{19}\text{F}$ -NMR in  $\text{CDCl}_3$ .

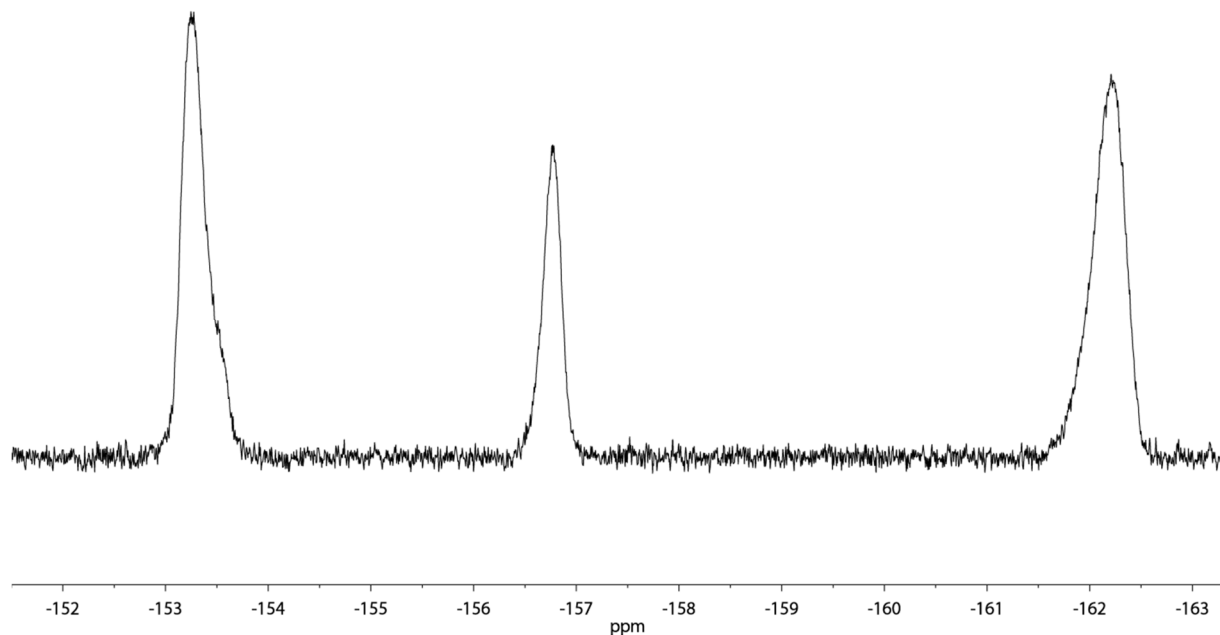
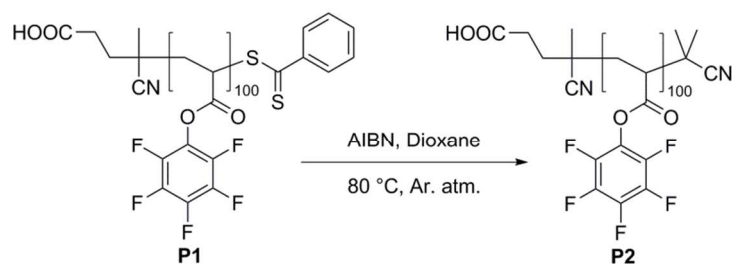


**Figure S5:** The  $^{19}\text{F}$ -NMR spectrum of **P1** in  $\text{CDCl}_3$ , after precipitation.

#### Endgroup modification of poly(pentafluorophenyl acrylate) (**P2**)<sup>S1</sup>



Polymer **P1** (6.5 g) and 2,2'-azobis(2-methylpropionitrile) (AIBN) (0.81 g, 4.91 mmol) were dissolved in anhydrous 1,4-dioxane (65 mL). The reaction mixture was degassed by bubbling argon for 30 minutes and subsequently immersed in a pre-heated oil bath at 80 °C. After five hours the mixture was cooled to room temperature and all volatiles were evaporated. The crude polymer was redissolved in a small amount of DCM and purified via precipitation in cold *n*-pentane (3 $\times$ ). Polymer **P2** was obtained as a white solid (5.98 g).

$^1\text{H}$ -NMR (400 MHz,  $\text{CDCl}_3$ ):  $\delta$  3.08 (br), 2.49 (br), 2.11 (br).

$^{19}\text{F}$ -NMR (376 MHz,  $\text{CDCl}_3$ ):  $\delta$  -153.2 (br), -156.8 (br), -162.2 (br).

SEC (THF):  $M_n = 12.8 \text{ kg mol}^{-1}$ ,  $D_M = 1.23$ .

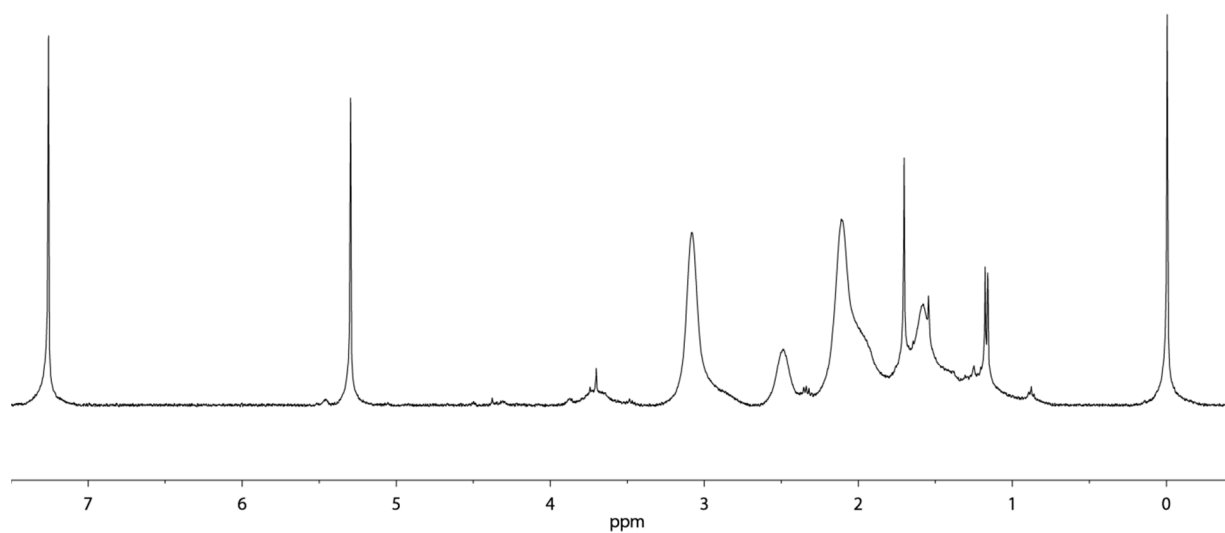


**Figure S6:** The  $^1\text{H}$ -NMR spectrum of **P2** in  $\text{CDCl}_3$ .

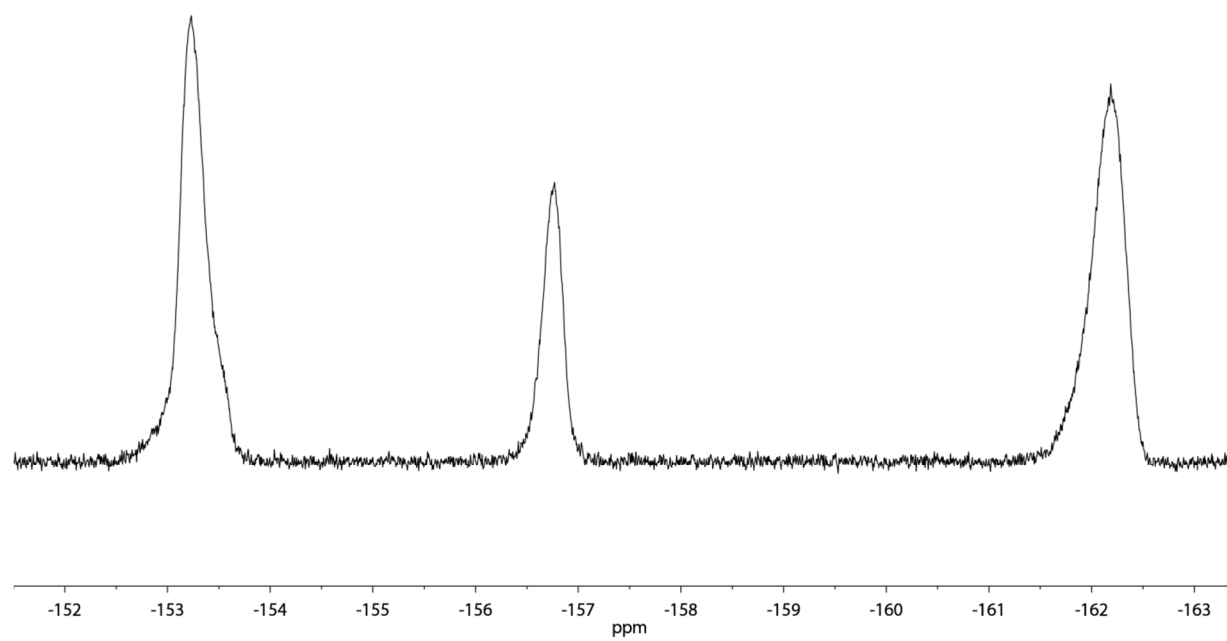
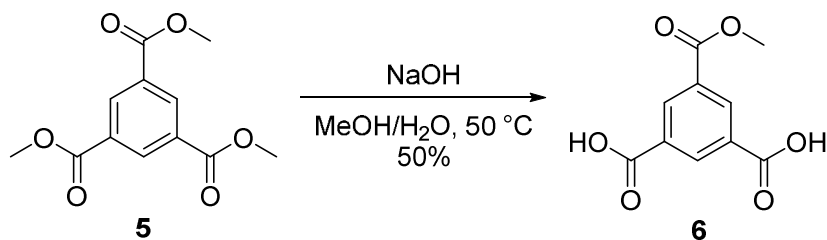


**Figure S7:** The  $^{19}\text{F}$ -NMR spectrum of **P2** in  $\text{CDCl}_3$ .

### Synthesis of 5-(methoxycarbonyl)isophthalic acid (**6**)



Trimethyl Benzene-1,3,5-tricarboxylate (**5**) (28.16 g, 112 mmol) was added to 350 mL MeOH. The formed suspension was heated to 50 °C while being stirred. Sodium hydroxide (9.41 g, 235 mmol) was dissolved in MeOH (350 mL) and slowly added to the reaction mixture using a dropping funnel. The conversion was monitored using <sup>1</sup>H-NMR. Upon reaching complete conversion the suspension was filtered over a glass filter and washed with MeOH (60 mL) and Et<sub>2</sub>O (125 mL). The methanol wash was concentrated using the rotavap and once again filtered and washed with MeOH and Et<sub>2</sub>O subsequently. The previous step was repeated once more. All the salts were combined and dissolved in H<sub>2</sub>O (220 mL). The solution was treated with 1 M HCl and the formed precipitate was collected via filtration and washed with H<sub>2</sub>O. The precipitate was dissolved in THF and impregnated in 70 g of silica. Product **6** was obtained as a white solid (12.49 g, 55.7 mmol, 50%) after purification using column chromatography (silica, elution: CHCl<sub>3</sub> : formic acid (99.5 : 0.05) -> CHCl<sub>3</sub> : THF : formic acid (83.5 : 16 : 0.5)).

<sup>1</sup>H-NMR (400 MHz, CDCl<sub>3</sub>): δ 8.80 (t, *J* = 1.9 Hz, 2H), 8.77 (d, *J* = 1.7 Hz, 1H), 3.98 (s, 3H).

<sup>13</sup>C-NMR (100 MHz, CDCl<sub>3</sub>): δ 167.79, 166.84, 135.66, 135.22, 133.29, 132.37, 53.11.



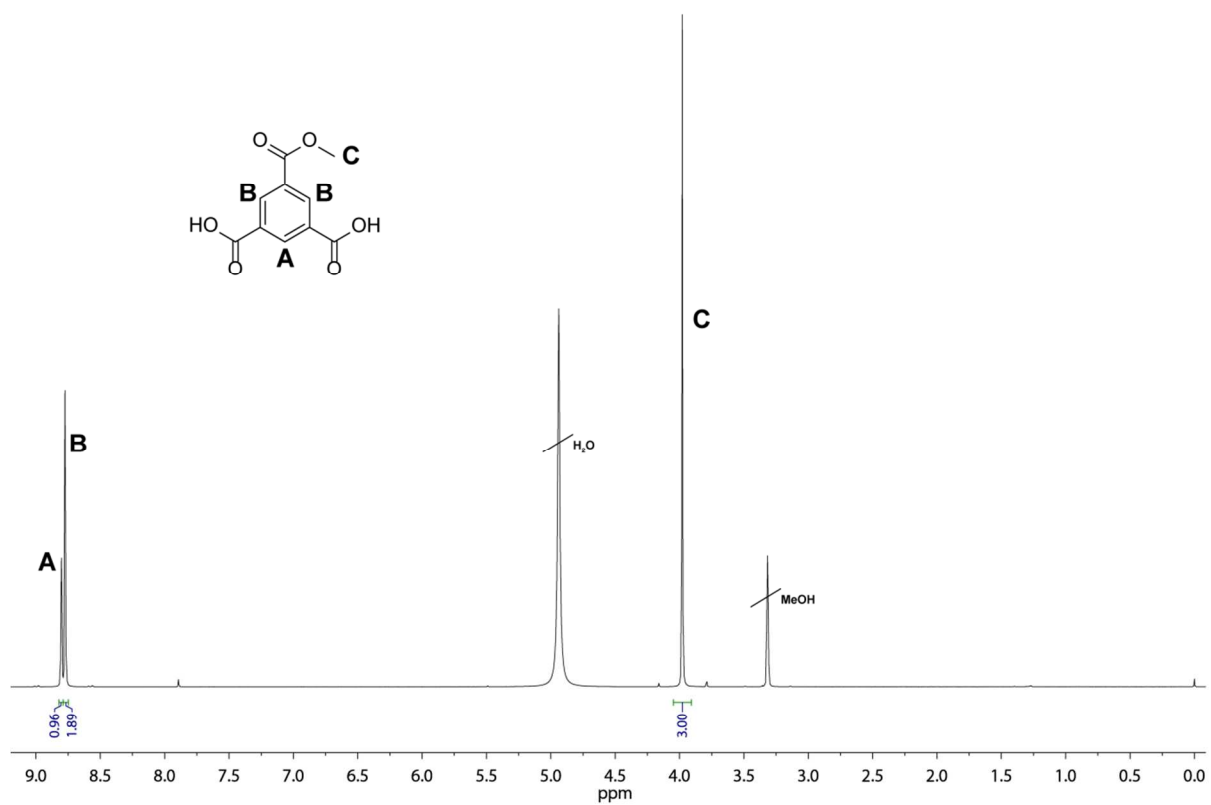


**Figure S8:** The  $^1\text{H-NMR}$  spectrum of **6** in MeOD.

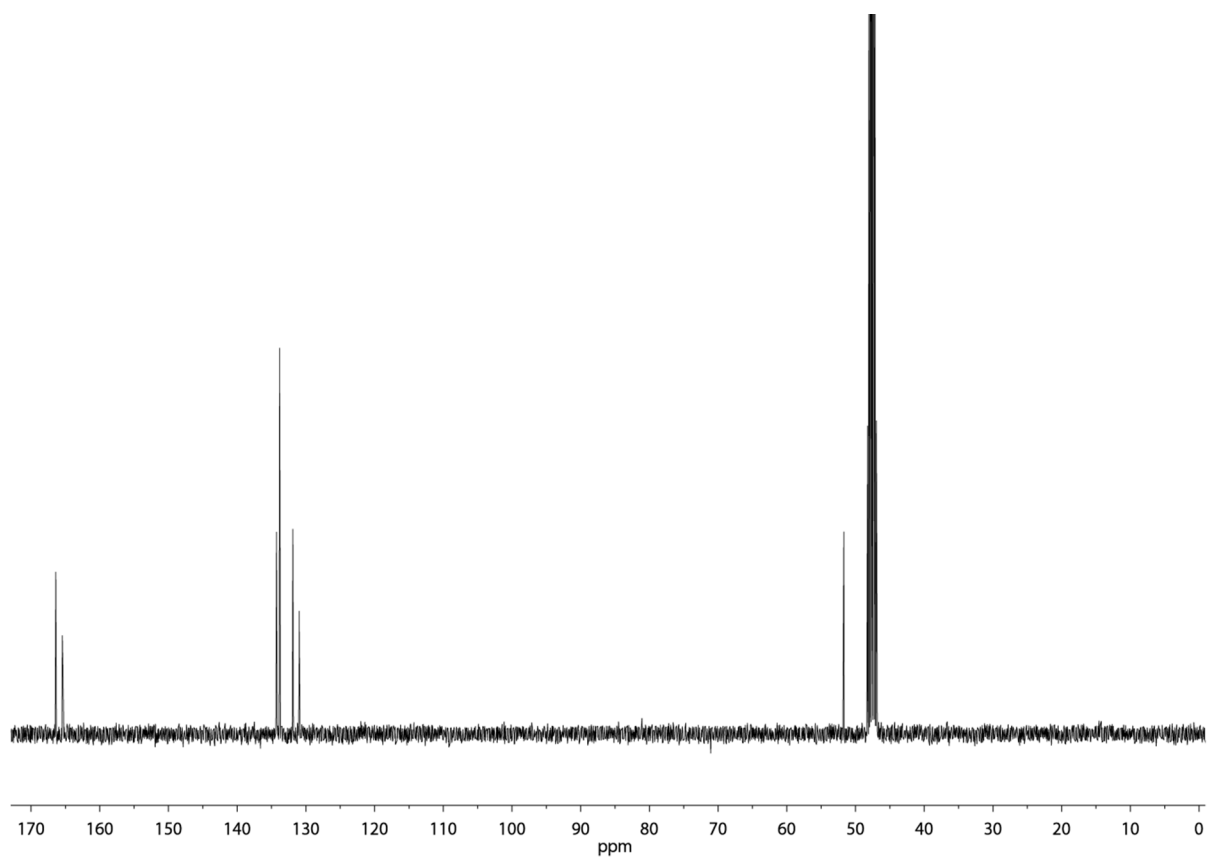
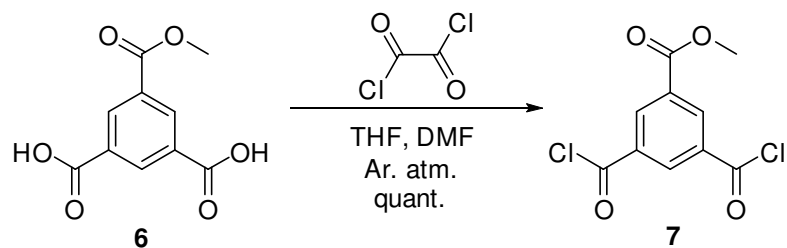


**Figure S9:** The  $^{13}\text{C-NMR}$  spectrum of **6** in MeOD.

### Synthesis of methyl 3,5-bis(chlorocarbonyl)benzoate (**7**)



Product **6** (5.01 g, 22.35 mmol) was dissolved in dry THF (35 mL). After the addition of one drop of DMF, the solution was cooled using an ice bath. Oxalyl chloride (5.52 mL, 63.0 mmol) was diluted with dry THF (35 mL) and added to the reaction mixture in a dropwise fashion using a dropping funnel (under an Argon atmosphere). The reaction mixture was allowed to slowly reach room temperature, and stirred until complete conversion was reached (the conversion was monitored using  $^1\text{H-NMR}$ ). All solvent was evaporated using the rotavap, followed by co-evaporating any remaining traces of water with toluene (2 $\times$ ). The product (**7**) was directly used in the next reaction step.

$^1\text{H-NMR}$  (400 MHz,  $\text{CDCl}_3$ ):  $\delta$  9.03 (d,  $J = 1.9$  Hz, 2H), 8.98 (t,  $J = 1.8$  Hz, 1H), 4.04 (s, 3H).

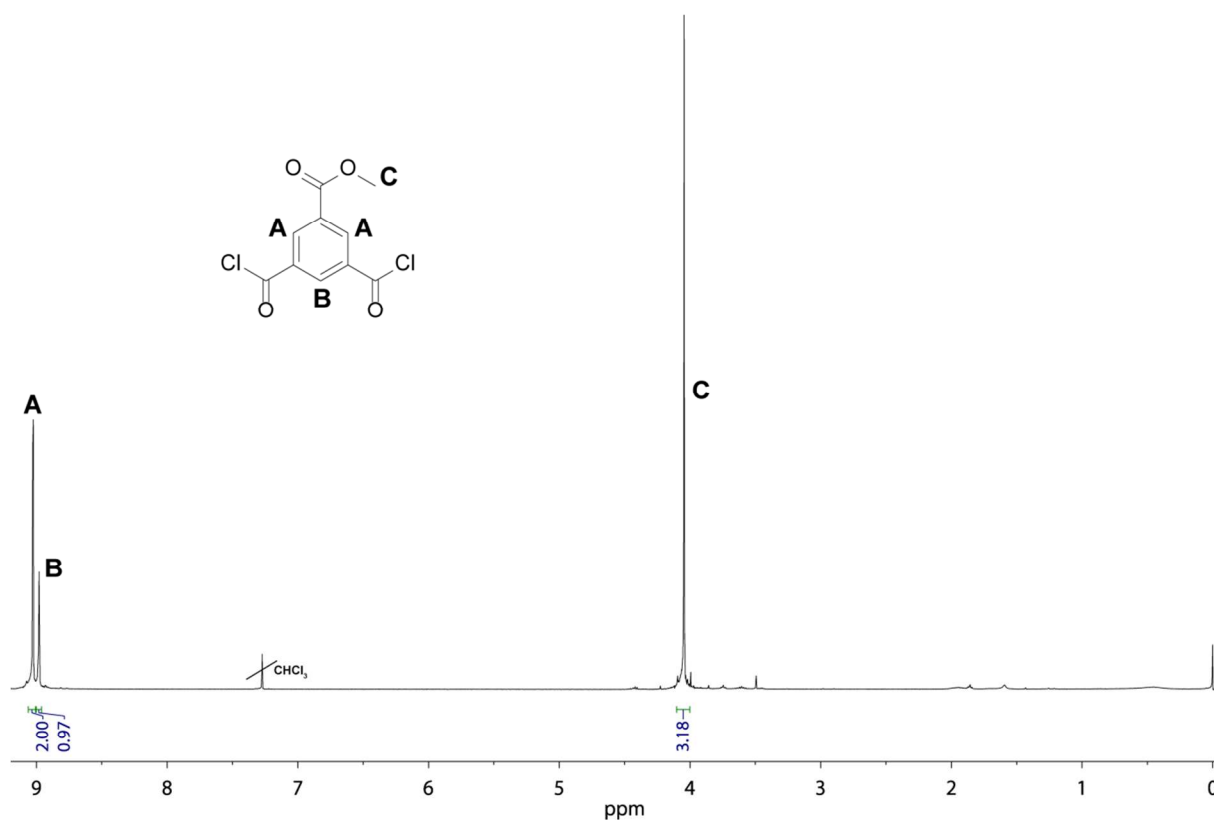
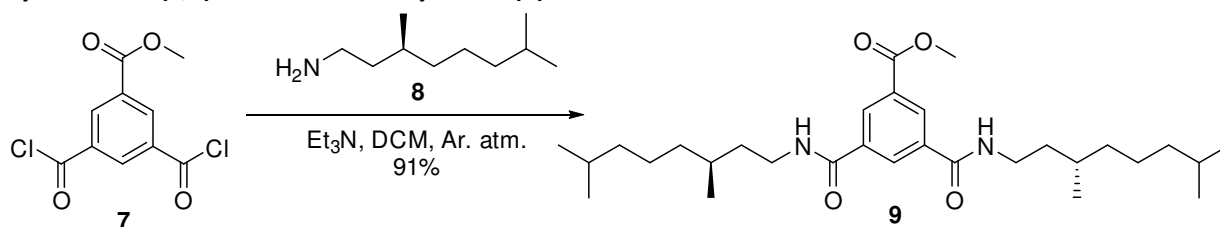


**Figure S10:** The  $^1\text{H-NMR}$  spectrum of **7** in  $\text{CDCl}_3$ .

### Synthesis of (*S,S*)-BDA monomethyl ester (**9**)



(*S*)-Dihydrocitronellyl amine (**8**) (7.37 g, 46.9 mmol) and triethylamine (10.9 mL, 78 mmol) were dissolved in dry DCM (25 mL). Product **7** (5.82 g, 22.29 mmol) was dissolved in dry DCM (25 mL) and added dropwise to the reaction mixture using a dropping funnel (under an argon atmosphere). The progress of the reaction was monitored using  $^1\text{H-NMR}$ . Upon reaching full conversion, the crude mixture was purified using column chromatography (silica, elution: 3% MeOH in DCM). Product **9** was obtained after evaporation of all volatiles (10.2 g, 20.3 mmol, 91%).

$^1\text{H-NMR}$  (400 MHz,  $\text{CDCl}_3$ ):  $\delta$  8.51 (d,  $J = 1.7$  Hz, 2H), 8.40 (t,  $J = 1.7$  Hz, 1H), 6.32 (t,  $J = 5.4$  Hz, 2H), 3.96 (s, 3H), 3.62 – 3.39 (m, 4H), 1.71 – 1.07 (m, 22H), 0.95 (d,  $J = 6.5$  Hz, 6H), 0.87 (d,  $J = 6.6$  Hz, 12H).

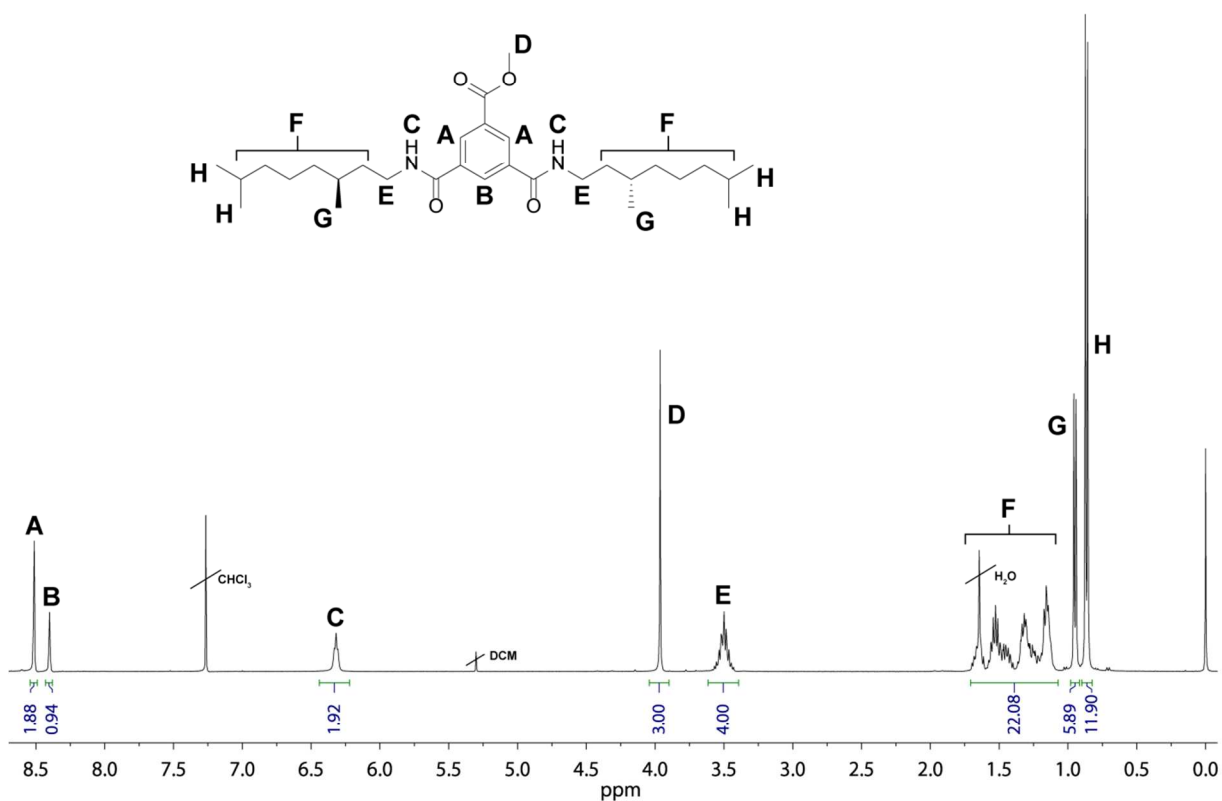
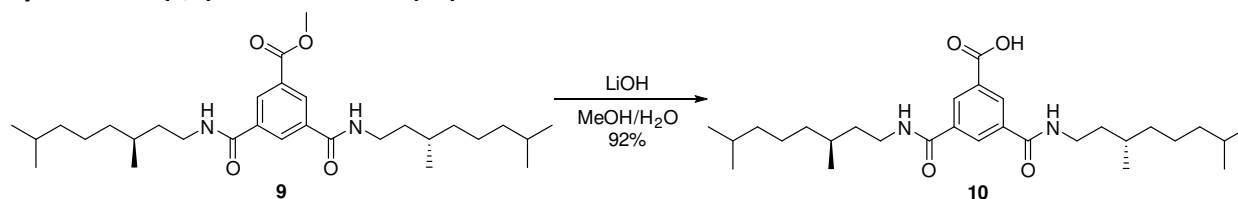


Figure S11: The  $^1\text{H-NMR}$  spectrum of **9** in  $\text{CDCl}_3$ .

### Synthesis of (*S,S*)-BDA monoacid (**10**)



Product **9** (10.19 g, 20.27 mmol) was dissolved in a mixture of MeOH (50 mL) and water (1.7 mL). LiOH (3.40 g, 142 mmol) was added and the reaction mixture was stirred overnight. The progress of the reaction was monitored via TLC using 4% MeOH in DCM as the elution. Upon reaching full conversion, the product was precipitated in 2 M HCl (750 mL). The formed solid was collected using a Büchner filter and washed with H<sub>2</sub>O (3 × 100 mL). Product **10** was obtained after drying the solid overnight in a vacuum oven at 60 °C (9.11 g, 16.6 mmol, 92%).

<sup>1</sup>H-NMR (400 MHz, CDCl<sub>3</sub>): δ 8.51 (d, *J* = 1.5 Hz, 2H), 8.33 (t, *J* = 1.7 Hz, 1H), 7.58 (t, *J* = 5.6 Hz, 1H), 3.54 – 3.40 (m, 4H), 1.74 – 1.06 (m, 20H), 0.95 (dd, *J* = 6.5, 1.2 Hz, 6H), 0.86 (dd, *J* = 6.6, 1.2 Hz, 12H).

<sup>13</sup>C-NMR (100 MHz, CDCl<sub>3</sub>): δ 168.98, 166.83, 134.96, 133.52, 130.69, 129.17, 39.19, 38.55, 38.41, 37.11, 36.38, 30.76, 27.88, 24.58, 22.57, 22.47, 19.35.

FT-IR (ATR): ν (cm<sup>-1</sup>) = 3313, 3074, 2954, 2925, 2869, 1699, 1642, 1593, 1537, 1446, 1406, 1381, 1366, 1290, 1258, 1228, 1182, 1143, 920, 806, 740, 711, 673.

MALDI-TOF-MS: *m/z* calc.: 488.7; found: 489.4 (*M* + H<sup>+</sup>), 495.4 (*M* + Li<sup>+</sup>), 511.4 (*M* + Na<sup>+</sup>).

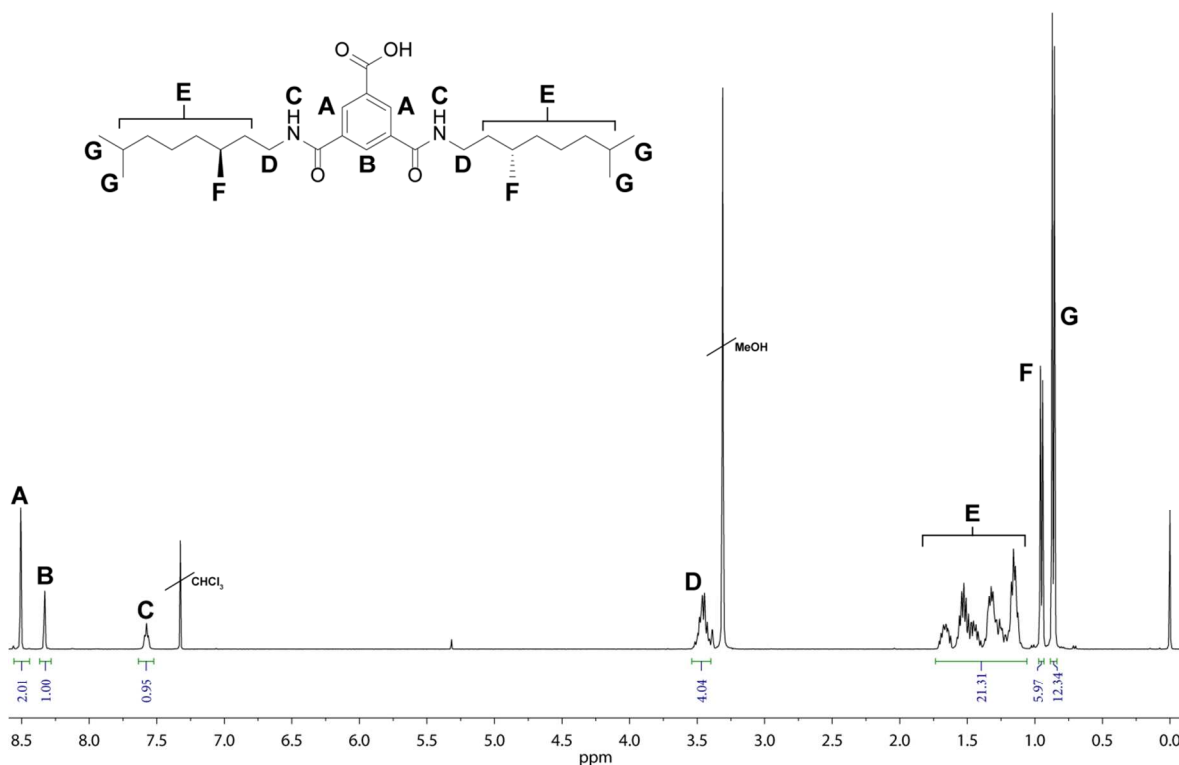


**Figure S12:** The <sup>1</sup>H-NMR spectrum of **10** in a mixture of CDCl<sub>3</sub> and MeOD.

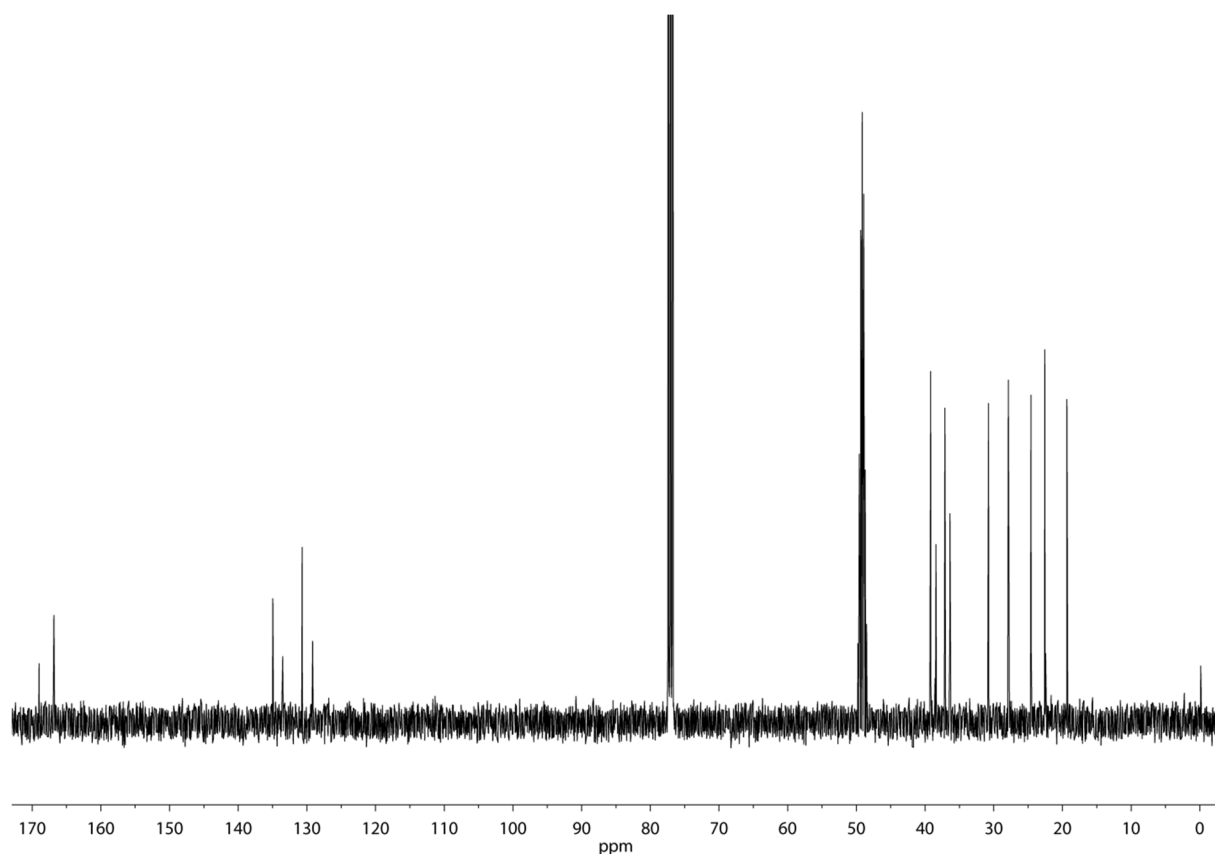
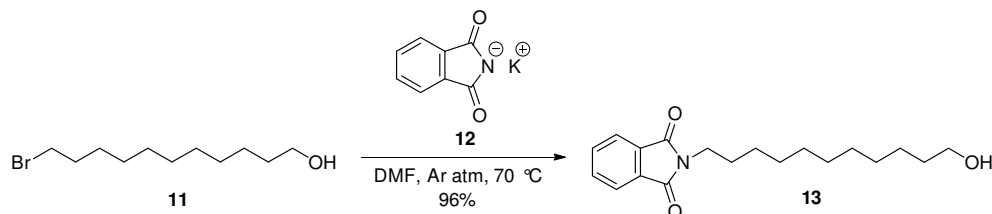


**Figure S13:** The  $^{13}\text{C}$ -NMR spectrum of **10** in a mixture of  $\text{CDCl}_3$  and MeOD.

### Synthesis of 1-undecanol-11-phthalimide (**13**)



The 11-bromo-1-undecanol (**11**) (25.27 g, 101 mmol) and phthalimide potassium salt (**12**) (24.27 g, 131 mmol) were dissolved in DMF (250 mL). The mixture was placed under an argon atmosphere and heated to 70 °C. The reaction was stirred for five hours after which the formed precipitate was removed via filtration. The residue was washed with EtOAc (800 mL) and the combined organic layer was washed with  $\text{H}_2\text{O}$  (4× 250 mL). After washing with a saturated KCl solution (2× 200 mL), the organic layer was dried over  $\text{MgSO}_4$ . Product **13** was obtained after all solvent was evaporated using the rotavap (30.8 g, 97.0 mmol, 96 %).

$^1\text{H}$ -NMR (400 MHz,  $\text{CDCl}_3$ ):  $\delta$  7.84 (dd,  $J = 5.5, 3.1$  Hz, 2H), 7.71 (dd,  $J = 5.4, 3.0$  Hz, 2H), 3.78 – 3.51 (m, 4H), 1.67 (p,  $J = 7.1$  Hz, 2H), 1.56 (m, 2H), 1.39 – 1.23 (m, 14H).

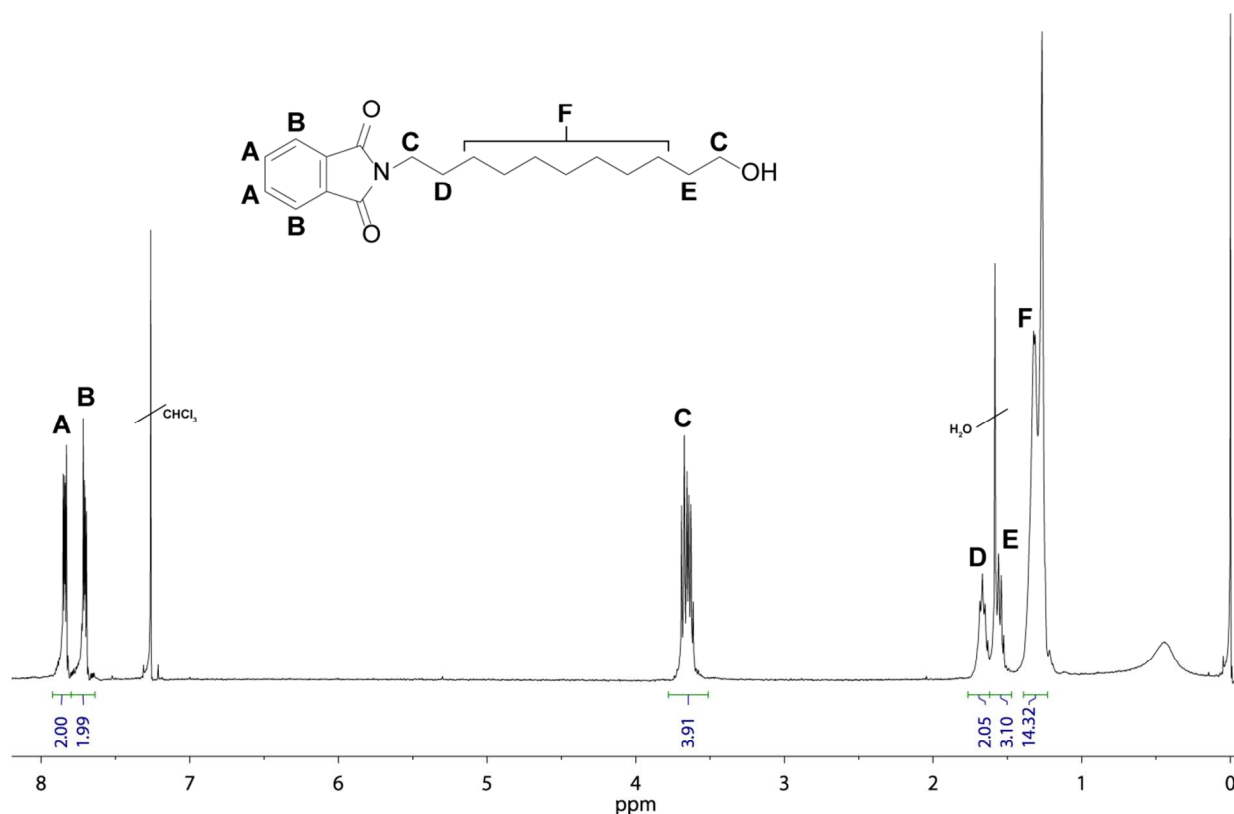
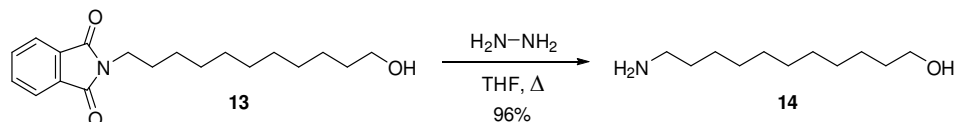


**Figure S14:** The  $^1\text{H}$ -NMR spectrum of **13** in  $\text{CDCl}_3$ .

#### Synthesis of 11-amino-1-undecanol (**14**)



The 1-undecanol-11-phthalimide (**13**) (30.79 g, 97 mmol) was dissolved in dry THF (570 mL). Hydrazine (80 mL, 2.55 mol) was added and the solution was refluxed. The yellow precipitate that formed during the reaction was removed via filtration. All solvent was evaporated using the rotavap, and the remaining solid was dissolved in  $\text{CHCl}_3$ . This solution was washed with 3 M NaOH (300 mL),  $\text{H}_2\text{O}$  (300 mL) and brine (300 mL) subsequently. The organic layer was dried over  $\text{MgSO}_4$  and all solvent was evaporated. Product **14** was obtained as a white powder (17.52 g, 94.0 mmol, 97 %).

$^1\text{H}$ -NMR (400 MHz,  $\text{CDCl}_3$ ):  $\delta$  3.64 (t,  $J$  = 6.6 Hz, 2H), 2.67 (t,  $J$  = 7.0 Hz, 2H), 1.63 – 1.21 (m, 18H).

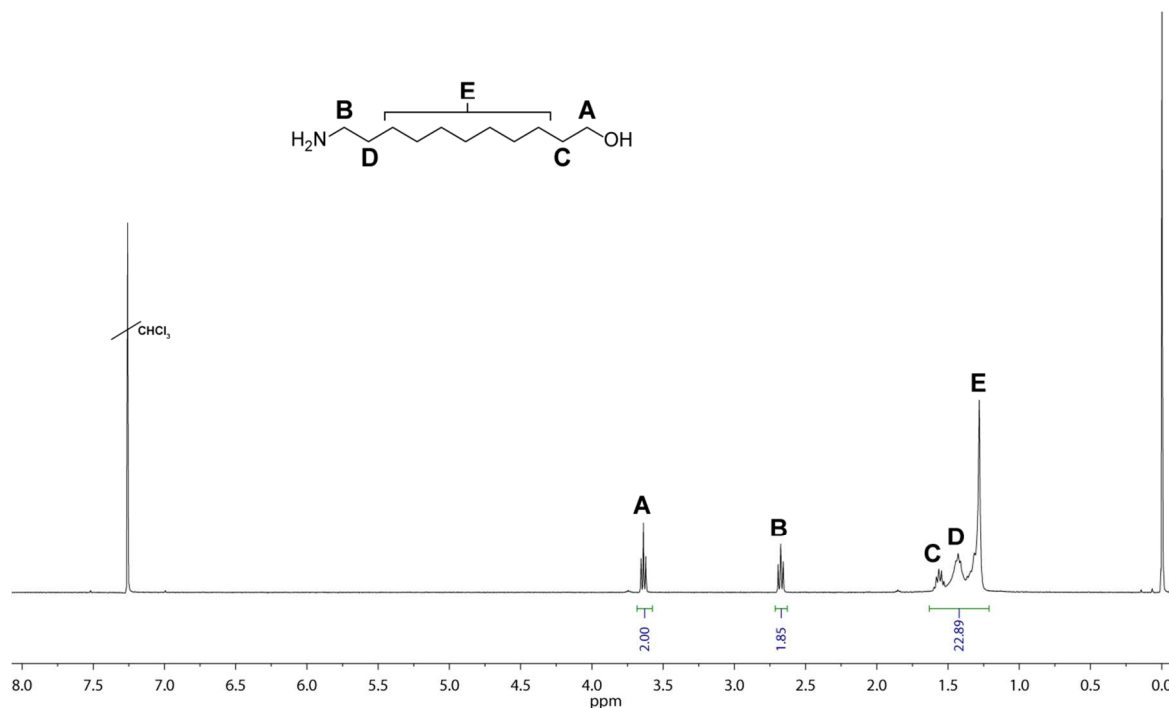
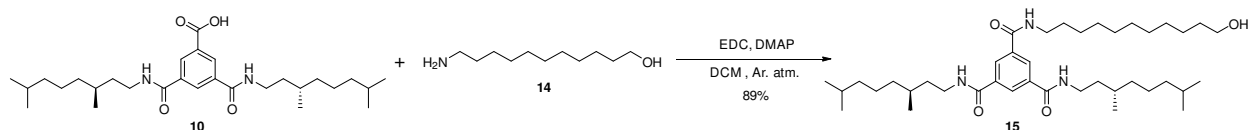


**Figure S15:** The  $^1\text{H}$ -NMR spectrum of **14** in  $\text{CDCl}_3$ .

### Synthesis of (*S,S*)-BTA- $\text{C}_{11}$ -OH (**15**)



The (*S,S*)-BTA-COOH (**10**) (2.51 g, 5.13 mmol), 11-amino-1-undecanol (**14**) (1.21 mL, 6.47 mmol) and DMAP (0.19 g, 1.58 mmol) were dissolved in 30 mL of dry DCM. *N*-(3-Dimethylaminopropyl)-*N'*-ethylcarbodiimide hydrochloride (EDC) (1.30 g, 6.78 mmol) was dissolved in 20 mL of dry DCM and added to the reaction mixture. The mixture was stirred over the weekend at room temperature while under an argon atmosphere. Full conversion was never reached, so the crude reaction mixture was directly purified via column chromatography (silica, elution: 4% MeOH in DCM). Product **15** was obtained after evaporation of the solvents using the rotavap and vacuum line (3.0 g, 4.56 mmol, 89%).

$^1\text{H}$ -NMR (400 MHz,  $\text{CDCl}_3$ ):  $\delta$  8.36 (d,  $J = 1.6$  Hz, 2H), 8.34 (t,  $J = 1.6$  Hz, 1H), 6.65 (t,  $J = 5.6$  Hz, 1H), 6.58 (t,  $J = 5.6$  Hz, 2H), 3.63 (q,  $J = 6.3$  Hz, 2H), 3.47 (m, 6H), 1.69 – 1.05 (m, 40H), 0.94 (d,  $J = 6.5$  Hz, 6H), 0.86 (d,  $J = 6.6$  Hz, 12H).

$^{13}\text{C}$ -NMR (100 MHz,  $\text{CDCl}_3$ ):  $\delta$  165.69, 135.25, 127.97, 63.00, 40.34, 39.24, 38.54, 37.13, 36.62, 32.77, 30.76, 29.44, 29.39, 29.28, 29.25, 29.11, 27.95, 26.85, 25.66, 24.63, 22.70, 22.60, 19.48.

FT-IR (ATR):  $\nu$  ( $\text{cm}^{-1}$ ) = 3462, 3242, 3074, 2953, 2924, 2854, 1687, 1556, 1463, 1382, 1366, 1296, 1146, 1057, 907, 796, 722, 691.

MALDI-TOF-MS:  $m/z$  calc.: 658.0; found: 658.6 ( $\text{M} + \text{H}^+$ ), 680.5 ( $\text{M} + \text{Na}^+$ ), 696.5 ( $\text{M} + \text{K}^+$ ).

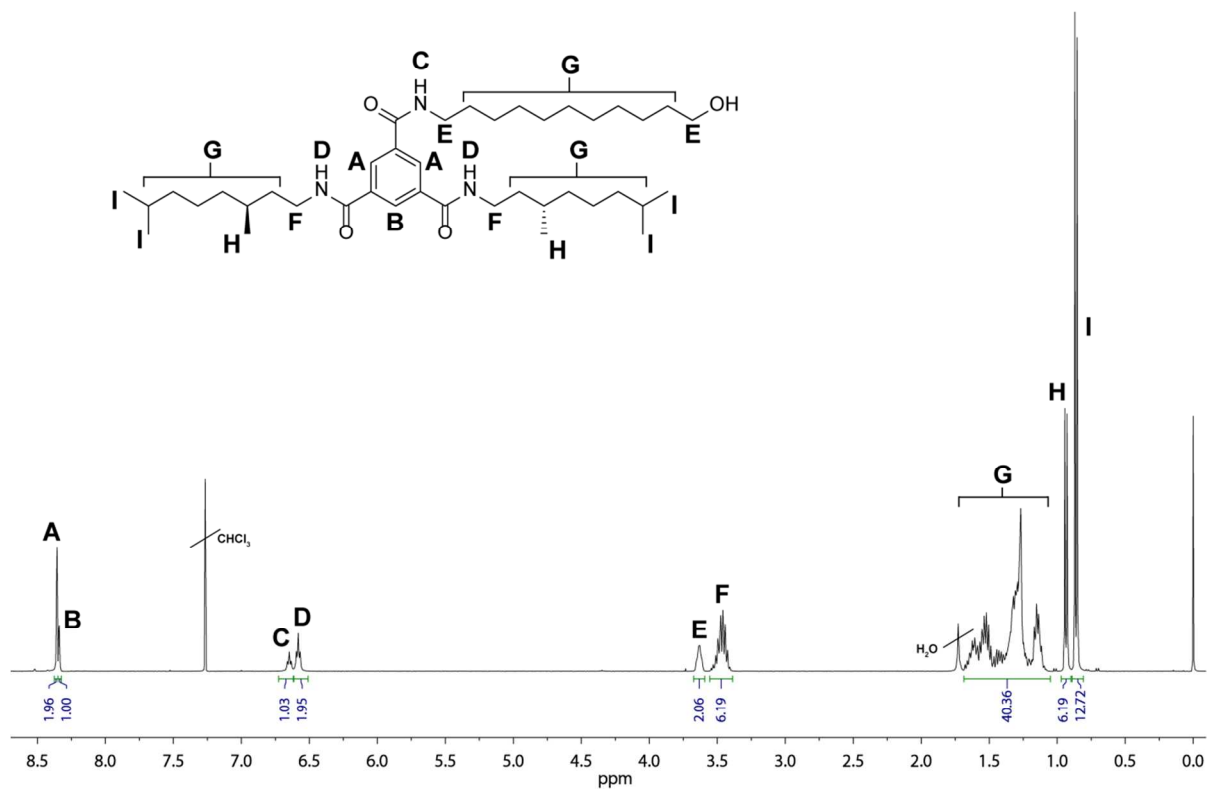


**Figure S16:** The  $^1\text{H-NMR}$  spectrum of **15** in  $\text{CDCl}_3$ .

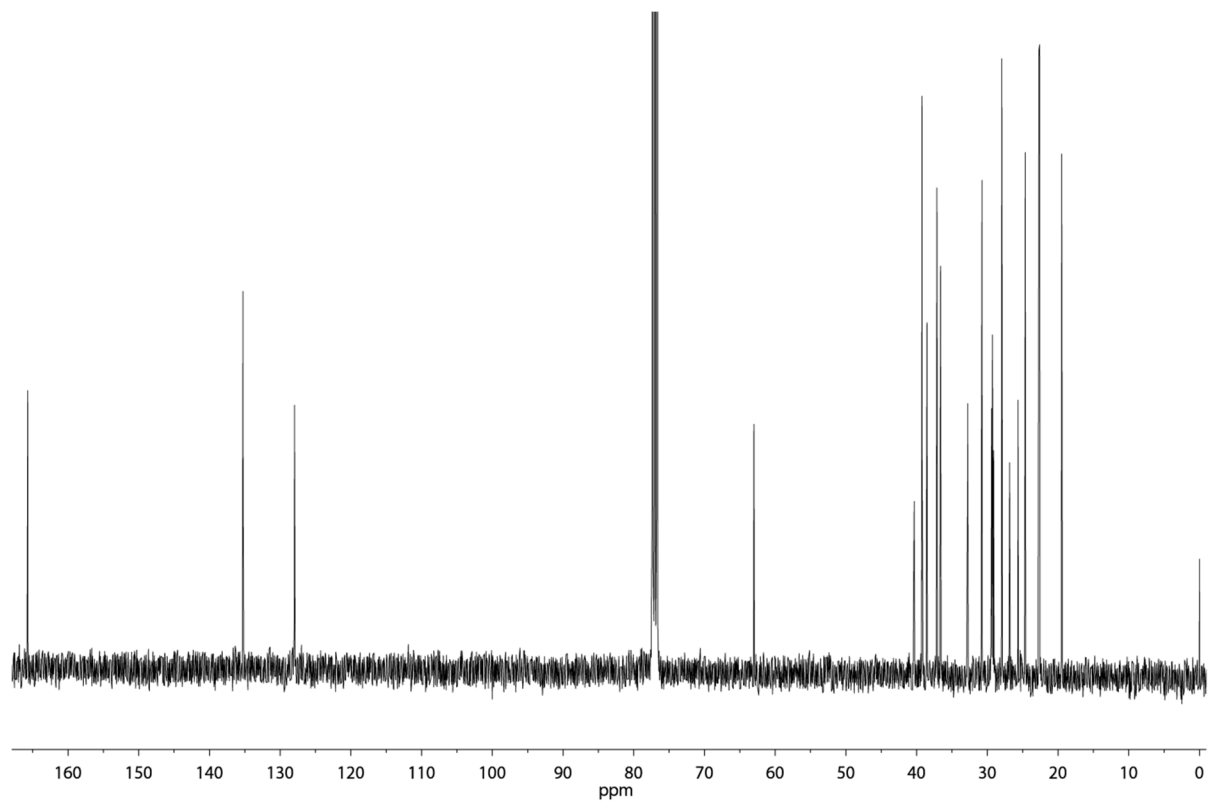
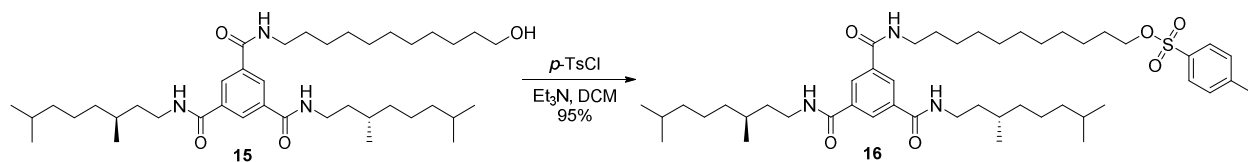


**Figure S17:** The  $^{13}\text{C-NMR}$  spectrum of **15** in  $\text{CDCl}_3$ .



### Synthesis of (*S,S*)-BTA-C<sub>11</sub>-tosylate (**16**)



The (*S,S*)-BTA-C<sub>11</sub>-OH (**15**) (5.74 g, 8.72 mmol) and triethylamine (2.1 mL, 15.07 mmol) were dissolved in 40 mL of dry DCM. The solution was cooled using an ice bath, before a solution of *p*-toluenesulfonyl chloride (1.85 g, 9.70 mmol) in dry DCM (10 mL) was added in a dropwise fashion. Upon reaching full conversion, the reaction mixture was washed with 1 M HCl (2×) and Brine (2×). After drying of the organic layer using MgSO<sub>4</sub>, the product was purified via column chromatography (silica, elution: DCM → 3% MeOH in DCM). Product **16** was obtained after evaporation of the solvents using the rotavap and vacuum line (6.70 g, 8.25 mmol, 95 %).

<sup>1</sup>H-NMR (400 MHz, CDCl<sub>3</sub>): δ 8.32 (d, *J* = 1.0 Hz, 3H), 7.80 – 7.75 (m, 2H), 7.35 – 7.31 (m, 2H), 6.66 (t, *J* = 5.7 Hz, 1H), 6.61 (t, *J* = 5.6 Hz, 2H), 4.00 (t, *J* = 6.5 Hz, 2H), 3.53 – 3.37 (m, 6H), 2.44 (s, 3H), 1.70 – 1.03 (m, 43H), 0.92 (dd, *J* = 6.5, 1.0 Hz, 6H), 0.85 (dd, *J* = 6.6, 1.0 Hz, 12H).

<sup>13</sup>C-NMR (100 MHz, CDCl<sub>3</sub>): δ 165.76, 135.22, 129.80, 128.02, 127.88, 70.73, 40.41, 39.25, 38.57, 37.13, 36.58, 30.76, 29.28, 28.85, 28.80, 27.95, 26.95, 25.29, 24.63, 22.71, 22.60, 21.64, 19.48.

FT-IR (ATR):  $\nu$  (cm<sup>-1</sup>) = 3237, 3071, 2925, 2855, 1724, 1638, 1557, 1462, 1364, 1298, 1188, 1176, 1123, 1098, 1035, 1012, 907, 814, 730, 691, 663, 555.

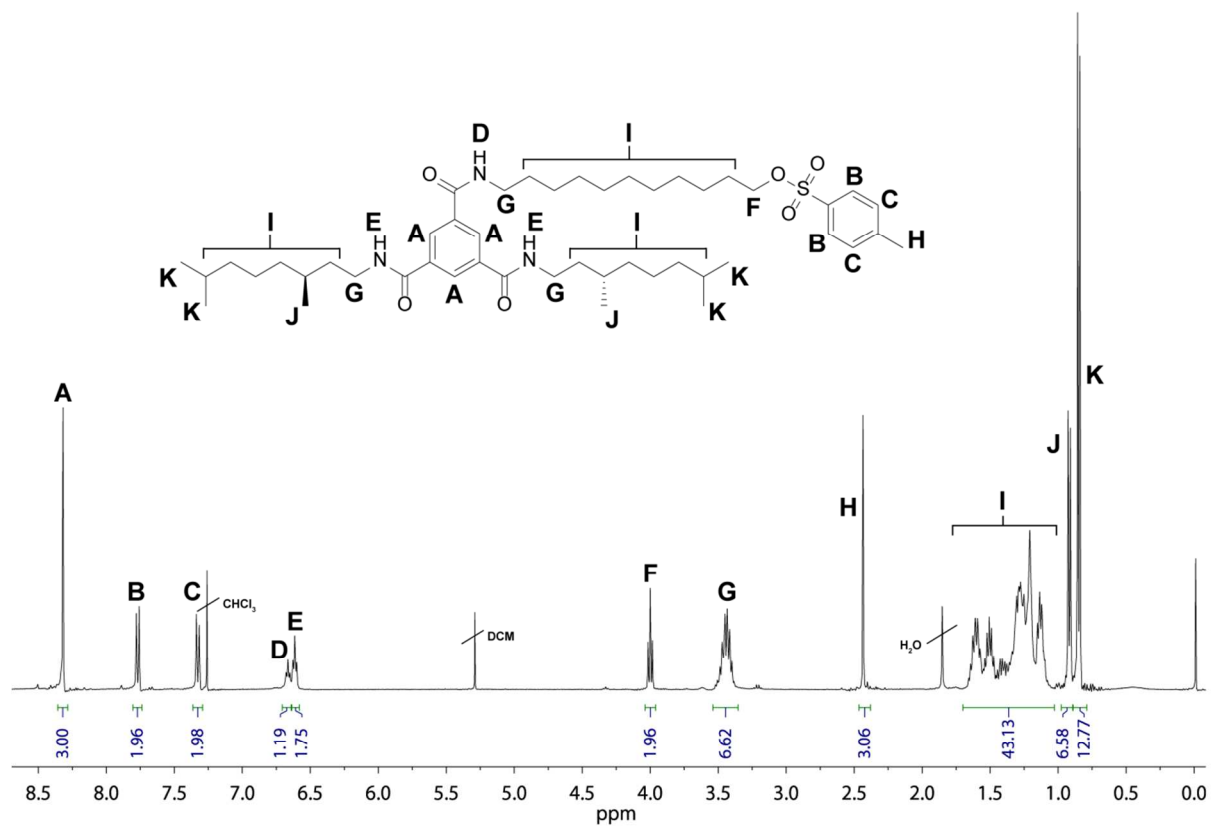


**Figure S18:** The  $^1\text{H-NMR}$  spectrum of **16** in  $\text{CDCl}_3$ .

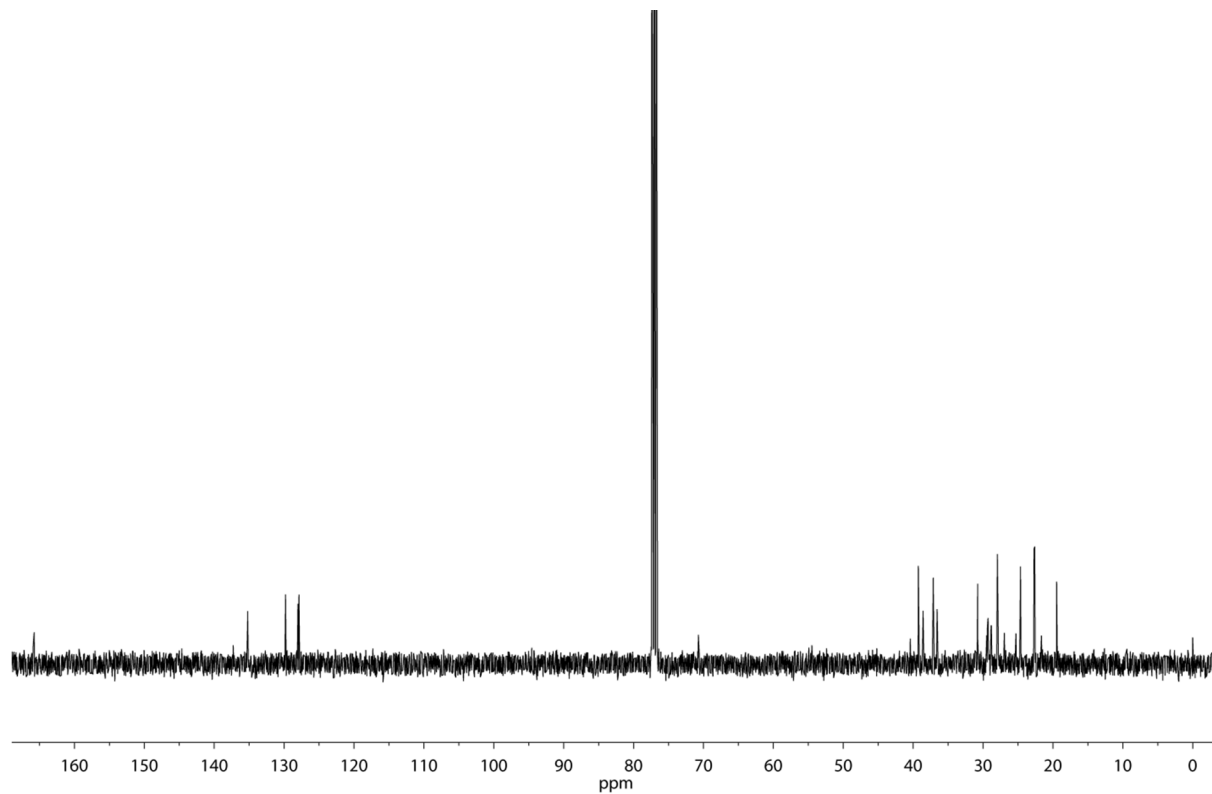
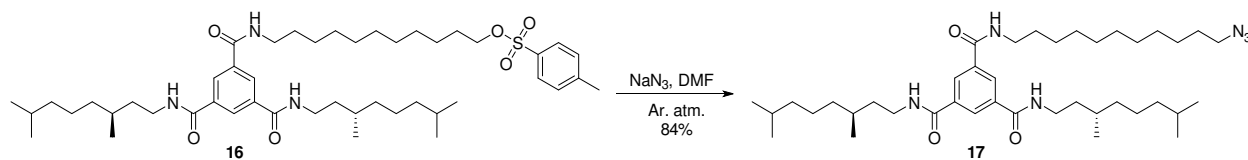


**Figure S19:** The  $^{13}\text{C-NMR}$  spectrum of **16** in  $\text{CDCl}_3$ .

### Synthesis of (*S,S*)-BTA-C<sub>11</sub>-N<sub>3</sub> (**17**)



The (*S,S*)-BTA-C<sub>11</sub>-tosylate (**16**) (6.70 g, 8.25 mmol) and sodium azide (1.0 g, 15.38 mmol) were dissolved in DMF (30 mL). The mixture was stirred overnight at room temperature while being kept under an argon atmosphere. Upon reaching full conversion (the conversion was monitored using <sup>1</sup>H-NMR), the reaction mixture was poured in ice water and the aqueous layer was extracted with EtOAc (4× 200 mL). The EtOAc layers were combined and subsequently washed with H<sub>2</sub>O (5× 200 mL) and dried over MgSO<sub>4</sub>. After filtration, all solvent was evaporated using the rotavap and the product was purified via column chromatography (silica, elution: 20% EtOAc in DCM). Product **17** was obtained as a white wax (4.73 g, 6.94 mmol, 84 %).

<sup>1</sup>H-NMR (400 MHz, CDCl<sub>3</sub>): δ 8.33 (s, 3H), 6.57 (t, *J* = 5.6 Hz, 1H), 6.53 (t, *J* = 5.6 Hz, 2H), 3.55 – 3.38 (m, 6H), 3.25 (t, *J* = 7.0 Hz, 2H), 1.70 – 1.03 (m, 42H), 0.93 (d, *J* = 6.5 Hz, 6H), 0.86 (d, *J* = 6.6 Hz, 12H).

MALDI-TOF-MS: *m/z* calc.: 683.0; found: 683.2 (M + H<sup>+</sup>), 705.6 (M + Na<sup>+</sup>), 721.5 (M + K<sup>+</sup>).

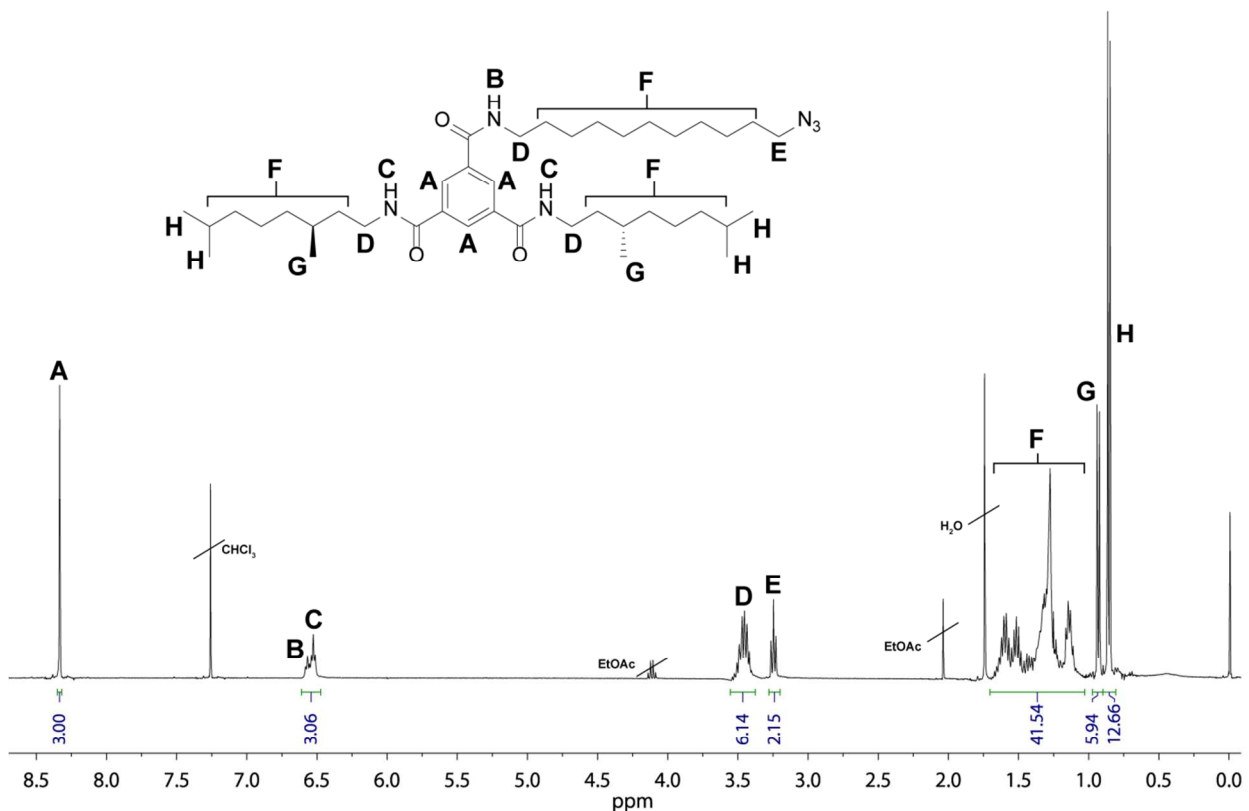
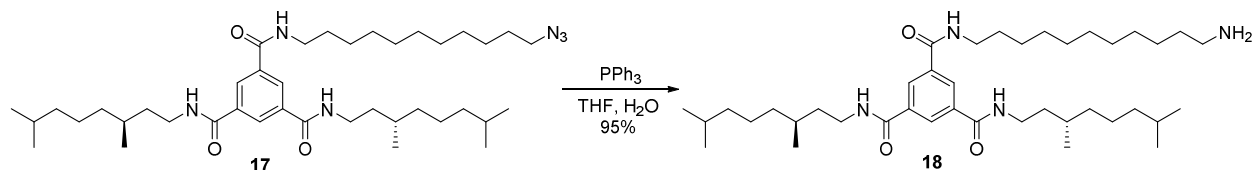


Figure S20: The <sup>1</sup>H-NMR spectrum of **17** in CDCl<sub>3</sub>.

### Synthesis of (*S,S*)-BTA-C<sub>11</sub>-NH<sub>2</sub> (**18**)



The (*S,S*)-BTA-C<sub>11</sub>-N<sub>3</sub> (**17**) (4.71 g, 8.25 mmol) was dissolved in a mixture of THF (55 mL) and water (6 mL). Triphenylphosphine (1.90 g, 7.24 mmol) was added to the solution, and the reaction mixture was stirred overnight. All solvent was evaporated using the rotavap and the crude, redissolved in DCM, was purified via column chromatography (silica, MeOH:DCM (4:96) → MeOH:DCM:Et<sub>3</sub>N (4:95:1)). Product **18** was obtained as a white wax (5.15 g, 7.84 mmol, 95 %).

<sup>1</sup>H-NMR (400 MHz, CDCl<sub>3</sub>): δ 8.34 (d, *J* = 1.5 Hz, 2H), 8.32 (t, *J* = 1.6 Hz, 1H), 7.32 (t, *J* = 5.7 Hz, 1H), 7.23 (t, *J* = 5.6 Hz, 2H), 3.50 – 3.30 (m, 6H), 3.10 (br, 3H), 2.71 (t, *J* = 7.1 Hz, 2H), 1.69 – 1.03 (m, 44H), 0.91 (d, *J* = 6.5 Hz, 6H), 0.85 (d, *J* = 6.6 Hz, 12H).

<sup>13</sup>C-NMR (100 MHz, CDCl<sub>3</sub>): δ 166.10, 166.08, 135.14, 135.12, 128.26, 41.69, 40.29, 39.25, 38.54, 37.16, 36.58, 32.39, 30.84, 29.36, 29.26, 29.21, 29.18, 29.05, 27.94, 26.85, 26.64, 24.64, 22.70, 22.59, 19.45.

FT-IR (ATR): ν (cm<sup>-1</sup>) = 3234, 3071, 2923, 2853, 1636, 1558, 1463, 1382, 1366, 1298, 1231, 1145, 1070, 906, 800, 731, 692.

MALDI-TOF-MS: *m/z* calc.: 657.0; found: 657.6 (M + H<sup>+</sup>), 679.6 (M + Na<sup>+</sup>).

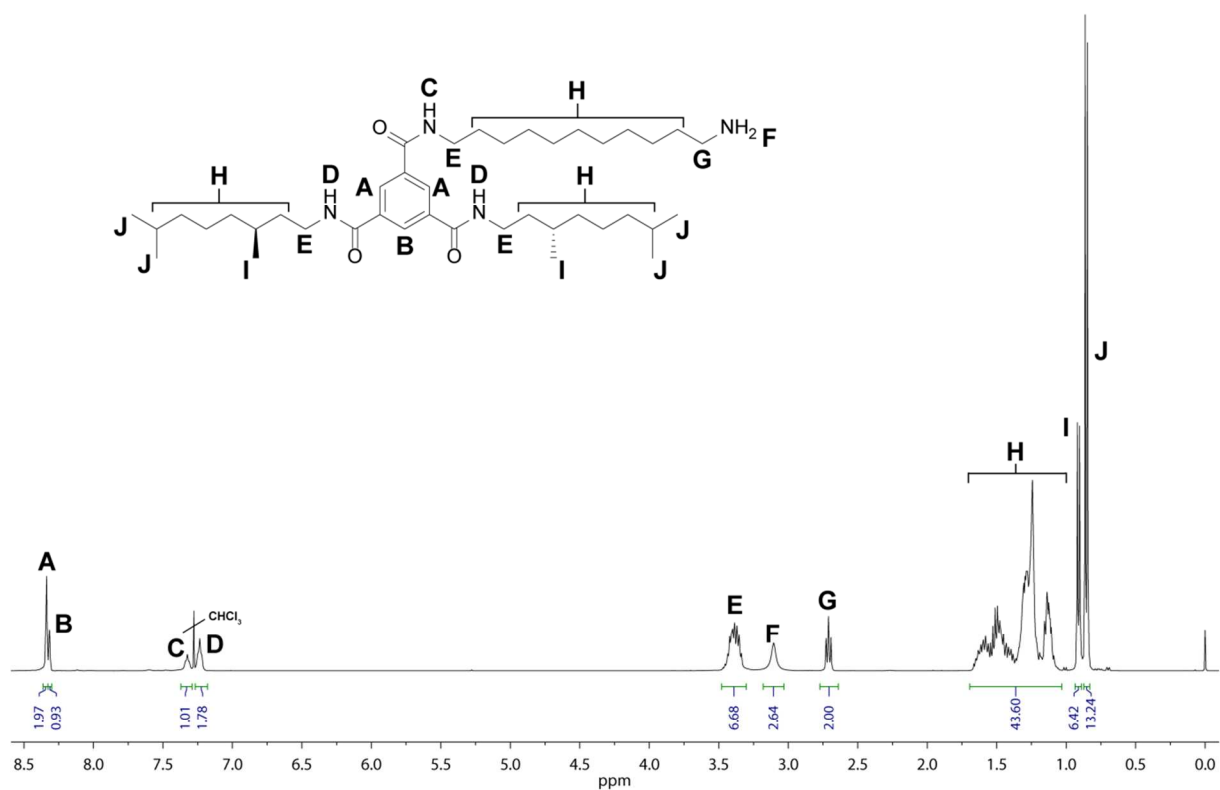


**Figure S21:** The  $^1\text{H-NMR}$  spectrum of **18** in  $\text{CDCl}_3$ .

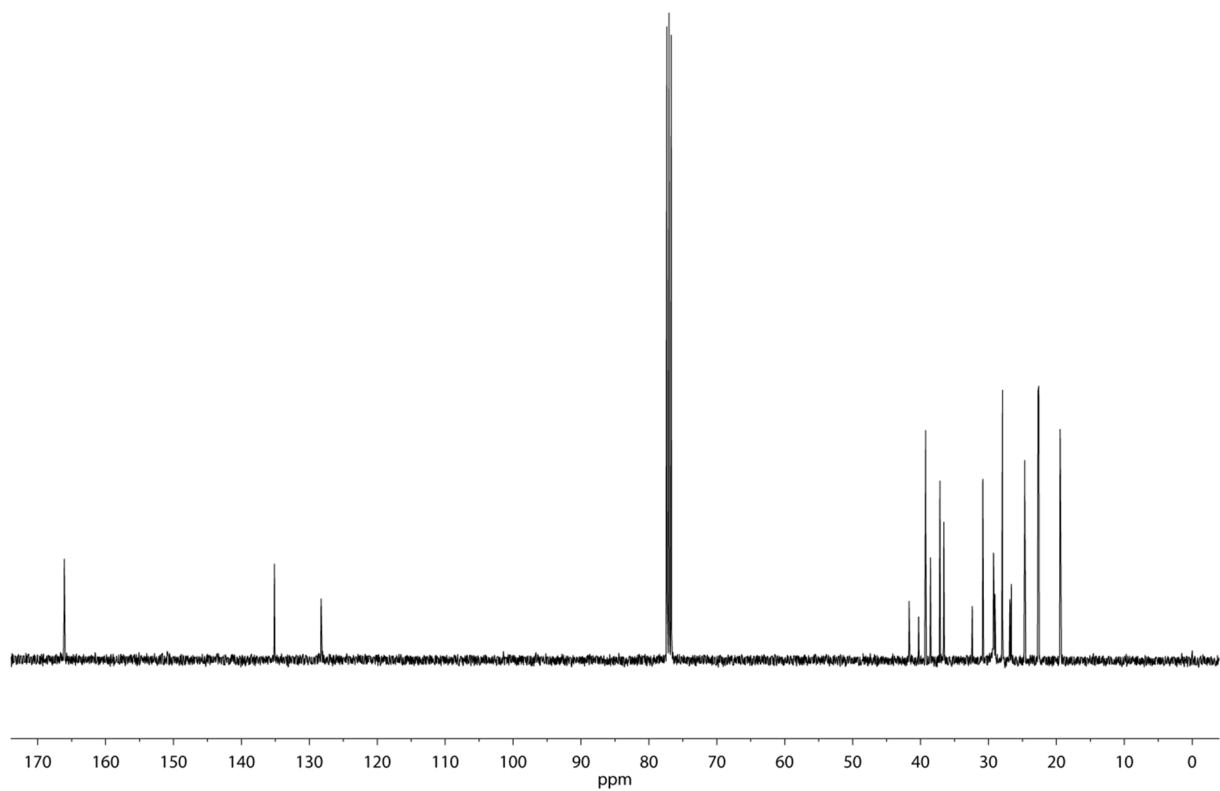
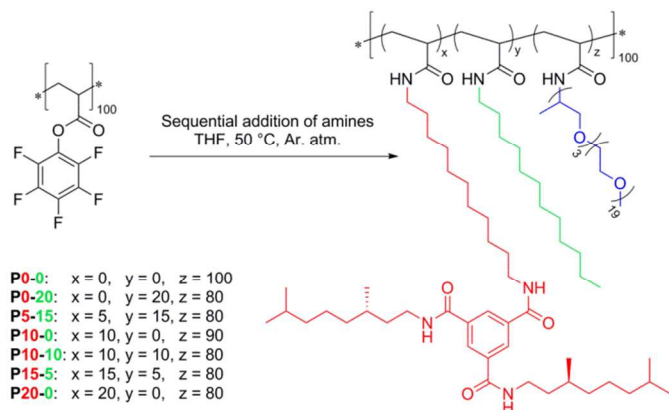


**Figure S22:** The  $^{13}\text{C-NMR}$  spectrum of **18** in  $\text{CDCl}_3$ .

## General post-functionalization procedure (P0-0, P0-20, P5-15, P10-0, P10-10, P15-5, P20-0)



The polymers were synthesized through sequential post-polymerization modification of **P2**. The general procedure is described as was performed for **P15-5**:

**P2** (60.0 mg, 2.5  $\mu\text{mol}$ , 1.0 eq.) was dissolved in 2 mL of dry THF. A solution of dodecylamine (2.33 mg, 12.6  $\mu\text{mol}$ , 5.0 eq.) in 2 mL of dry THF was added to the flask and the mixture was stirred at 50 °C under an argon atmosphere for one hour. Next, BTA-C<sub>11</sub>-amine (**18**) (24.8 mg, 37.7  $\mu\text{mol}$ , 15.0 eq.) dissolved in 2 mL of dry THF was added to the reaction mixture and stirred for 1 h. Finally, pre-dried Jeffamine M-1000 (400 mg, 383.8  $\mu\text{mol}$ , 150 eq.) dissolved in 4 mL of dry THF was added to the mixture and stirred at 50 °C overnight. The reaction mixture was first dialyzed in THF, followed by dialysis in methanol to remove the pentafluorophenol and the excess of Jeffamine. The polymer was obtained via precipitation from CHCl<sub>3</sub> into cold *n*-pentane and dried using high vacuum.

The conversion of the various post-functionalization steps was monitored using <sup>19</sup>F-NMR spectroscopy (Figure S23). Hereto, a sample was taken after each reaction step. After determining the degree of functionalization using <sup>19</sup>F-NMR spectroscopy, the sample's solvent was evaporated under reduced pressure, redissolved in dry THF and added back to the reaction mixture. Note: Since the mass of the added compounds has a direct influence on the functionalization percentages of the polymeric backbone, care should be taken during the weighting and addition process. The order of addition was chosen based on the desired incorporation percentages as well as the bulkiness of the various amines. Adding 80–90 mol% of Jeffamine M-1000 first would result in a relative long period of time of reaching full conversion because this group is the most bulky and abundantly incorporated amine. In addition, its incorporation would reduce the accessibility of reactive sites on the polymer and thereby reduce the rate of reaction of subsequent post-functionalization steps. Therefore, we added a 150-fold excess of Jeffamine M-1000 during the final step to reach full conversion within a reasonable period of time. Hence, the less bulky and abundantly incorporated amines (that is, BTA-C<sub>11</sub>-NH<sub>2</sub> and dodecylamine) were added first. Here, the order of incorporation does not matter as long as a solvent is used in which all components are molecularly dissolved.

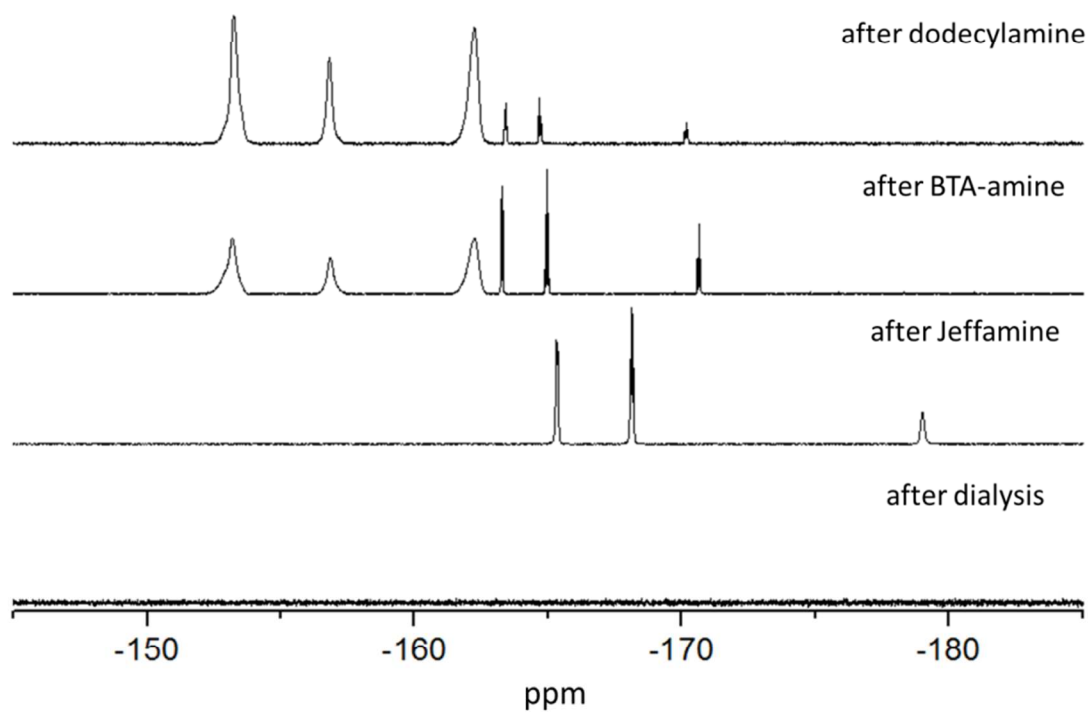


**Figure S23:** The  $^{19}\text{F}$ -NMR spectra of the sequential post-polymerization of **P2** into **P15-5**.

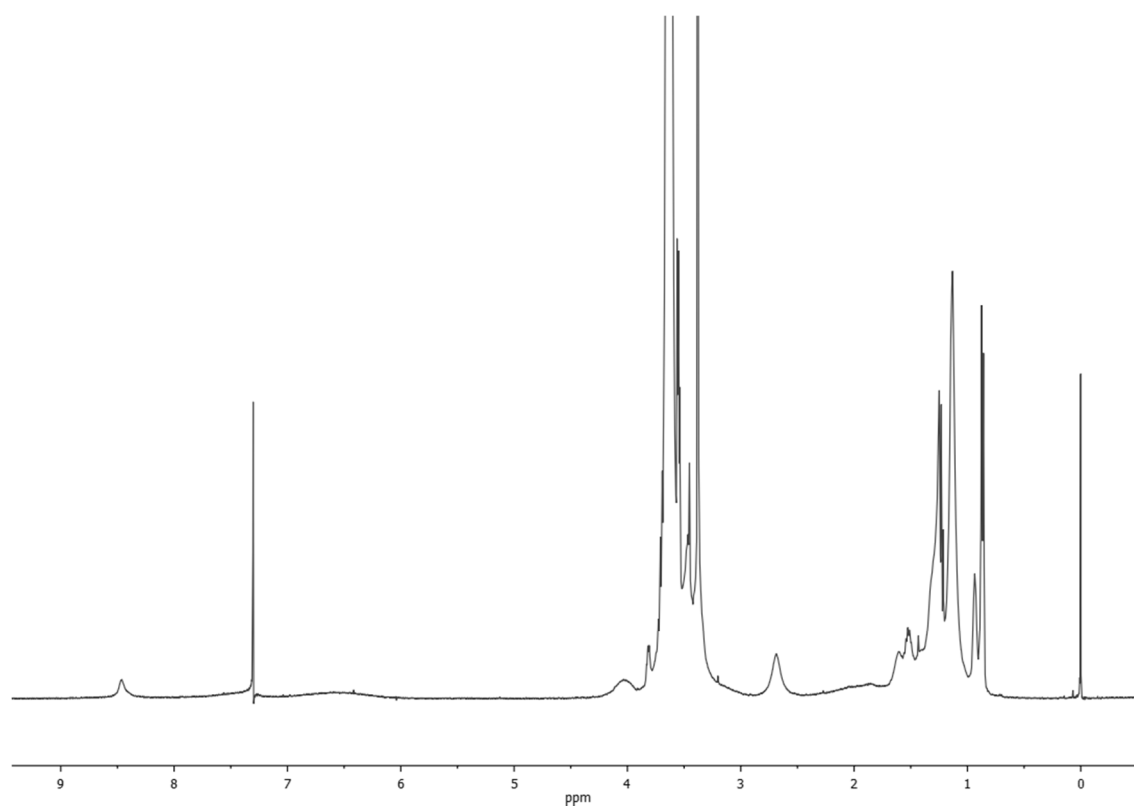


**Figure S24:** The  $^1\text{H}$ -NMR spectra of **P15-5** in  $\text{CDCl}_3$ .

#### 4. Sample preparation procedure

The following protocol was used to prepare aqueous solution of the various polymers:

- The polymer was dried overnight in a vacuum oven at 45 °C in the presence of phosphorus pentoxide ( $P_2O_5$ ).
- The desired amount of dried polymer was diluted with the corresponding amount of deionized water.
- The sample was sonicated for 45 minutes using a sonication bath.
- The sonicated sample was transferred directly to a preheated oven at 90 °C and heated for 45 minutes.
- The glass vial was allowed to cool to room temperature and equilibrate overnight.

It was anticipated that the sample preparation protocol affects the self-assembly of the BTA grafts. There, four different procedures were tested consisting of two steps of sonication or heating at 80 °C for 30 min. (Table S1 and Figure S25).

**Table S1:** Overview of the procedures employed to prepare aqueous solution of **P20-0**, which consist of two steps of sonication or heating at 80 °C for 30 min. The procedures are denoted according to the sequence of steps.

Procedure	Initial step (30 min.)	Sequential step (30 min.)
SH	Sonication	Heating at 80 °C
S	Sonication	Sonication
HS	Heating at 80 °C	Sonication
H	Heating at 80 °C	Heating at 80 °C

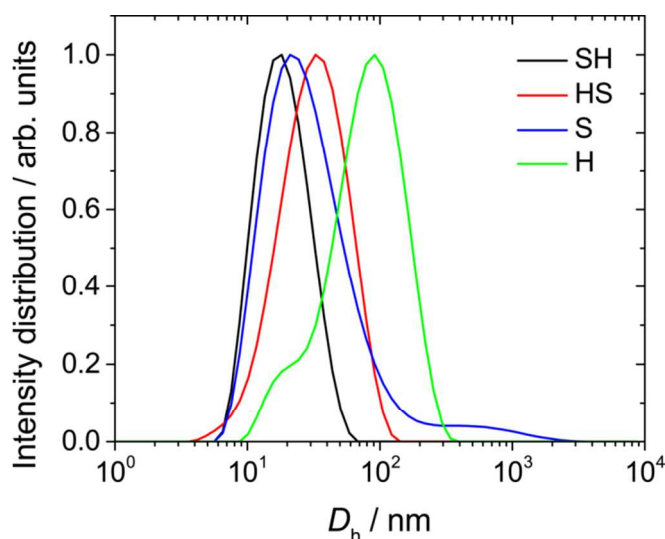


**Figure S25:** The intensity distribution of the hydrodynamic diameter ( $D_h$ ) of **P20-0** prepared according to different sample procedures ( $T = 20$  °C,  $c_{\text{polymer}} = 1$  mgmL $^{-1}$ ).



## 5. Dynamic and static light scattering

Measurements were performed on an ALV Compact Goniometer System (CGS-3) Multi-Detector (MD-4) equipped with an ALV-7004 Digital Multiple Tau Real Time Correlator and a laser of 532 nm. The scattering intensity was collected at scattering angles ( $\theta$ ) ranging from 40 to 140° in steps of 10°, and averaged over 3 runs of 30 seconds per angle. Samples were filtered using Anopore® syringe filters with pores of 0.1  $\mu\text{m}$  and held in disposable tubes of glass with an outer diameter of 10 mm. The absolute scattering intensity or Rayleigh ratio ( $R_\theta$ ) was computed according to equation S1.

$$R_\theta = \frac{I_s - I_{\text{sol}}}{I_{\text{tol}}} \cdot \left(\frac{n_{\text{sol}}}{n_{\text{tol}}}\right)^2 \cdot R_{\theta, \text{toluene}} \quad (\text{equation S1})$$

With  $I_s$ ,  $I_{\text{sol}}$ , and  $I_{\text{tol}}$  being the measured scattering intensities of the sample, solvent, and toluene, the refractive indices  $n_{\text{sol}}$  (= 1.33) and  $n_{\text{tol}}$  (= 1.49), and Rayleigh ratio of toluene ( $R_{\theta, \text{toluene}} = 2.1 \times 10^{-5} \text{ cm}^{-1}$  at 532 nm).<sup>S2</sup> Intensity cross-correlation functions ( $g^{(2)}(\tau)$ ) were measured at scattering vectors  $q$ , defined as in equation S2.

$$q = \frac{4 \cdot \pi \cdot n_{\text{sol}}}{\lambda} \cdot \sin\left(\frac{\theta}{2}\right) \quad (\text{equation S2})$$

Sequentially, the electric field cross-correlation functions ( $g^{(1)}(\tau)$ ) were calculated according to the Siegert equation (Equation S3) and analyzed with the CONTIN algorithm to determine distributions of the relaxation times ( $\tau_D$ ).

$$g^{(1)}(\tau) = \sqrt{g^{(2)}(\tau) - 1} \quad (\text{equation S3})$$

The apparent diffusion constant  $D_{\text{app}}$  was determined from the slope of the obtained relaxation times  $\tau_D$  versus  $q^2$ . (Figure S26A–G). Subsequently, the hydrodynamic radius ( $R_H$ ) was determined using the Stokes–Einstein relationship (equation S4). This formula contains the Boltzmann constant ( $k_B$ ), temperature ( $T$ ), viscosity ( $\eta$ ) and diffusion coefficient ( $D$ ).

$$R_H = \frac{k_B \cdot T}{6 \cdot \pi \cdot \eta \cdot D} \quad (\text{equation S4})$$

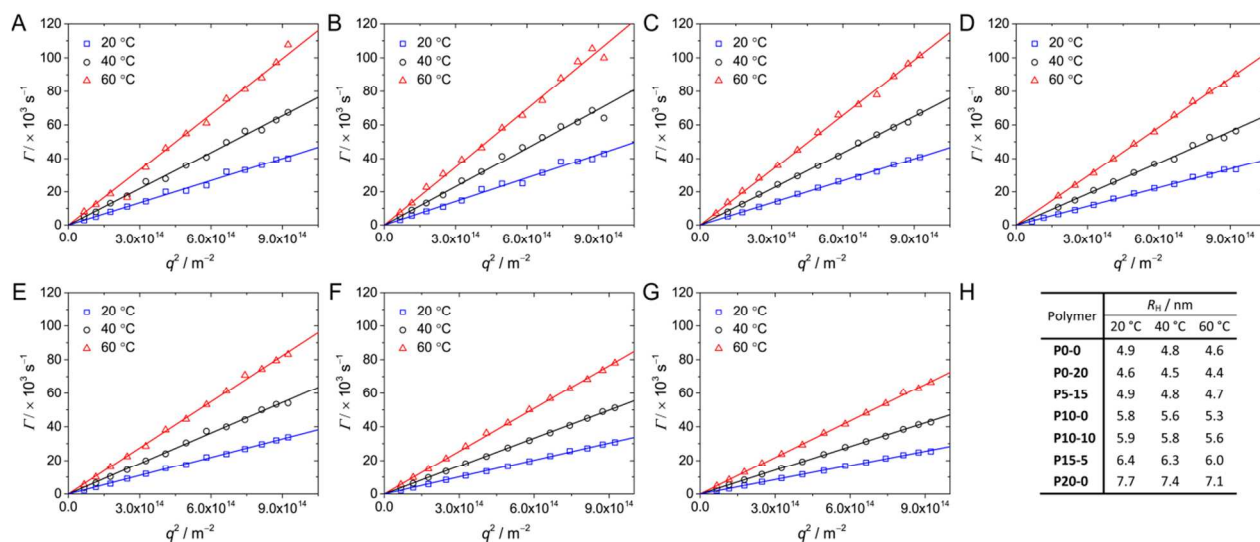


**Figure S26:** The angular dependence of the decay rate ( $\Gamma$ ) used to determine the apparent diffusion constant ( $D_{app}$ ) and the corresponding hydrodynamic radii ( $R_H$ ) ( $c_{polymer} = 1 \text{ mg mL}^{-1}$ ). A) P0-0, B) P0-20, C) P5-15, D) P10-0, E) P10-10, F) P15-5, G) P20-0, H) The corresponding  $R_H$  as function of temperature.

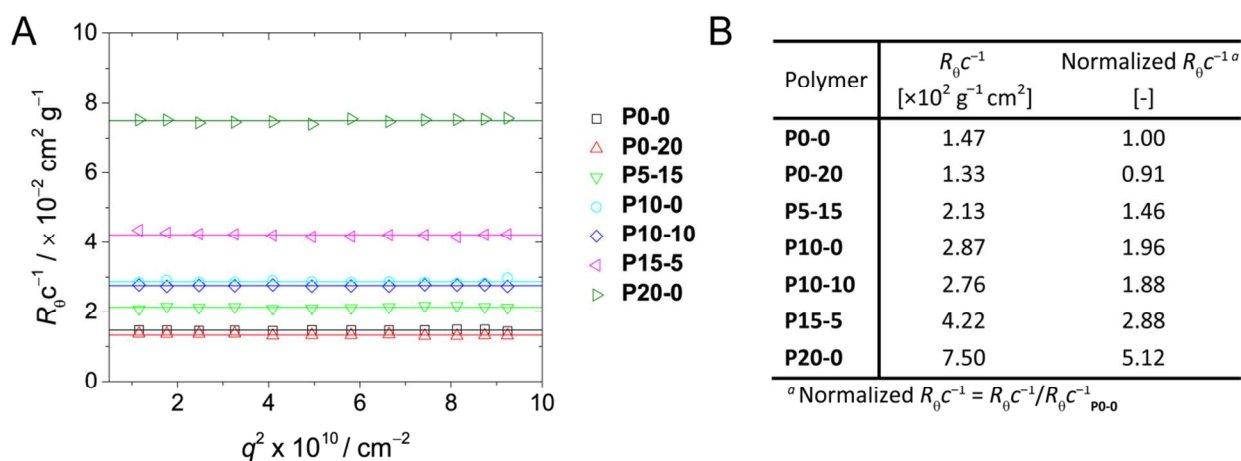


**Figure S27:** A) The angular dependence of the absolute scattering intensity ( $R_\theta$ ) corrected for the polymer concentration ( $c$ ) ( $c_{polymer} = 1 \text{ mg mL}^{-1}$ ), B) the average values of the absolute scattering intensity determined via a linear fit.

For all of the polymers, the average value of  $R_\theta$  proved to be independent of  $q$  within the measured range of values (Figure S27A). The angle-independence of the scattering intensity indicates that the sizes of the polymeric nanoparticles in solution were smaller than  $\lambda/20 \text{ nm}$  ( $\approx 27 \text{ nm}$ , where  $\lambda$  is the wavelength of the laser light). This is in line with the values obtained for the hydrodynamic radius ( $R_H$ ) of the nanoparticles via DLS (Figure S26H).

The angular dependence of the absolute scattering intensity or Rayleigh ratio ( $R_\theta$ ) of a dilute polymer solution at concentration ( $c$ ) relates to the weight-average molecular mass ( $M_w$ ), radius of gyration ( $R_g$ ) and the second virial coefficient ( $A_2$ ).

$$\frac{Kc}{R_\theta} = \frac{1}{M_w} \left( 1 + \frac{\langle R_g^2 \rangle q^2}{3} \right) + 2A_2c \text{ (equation S5)}$$

$$\text{Using } K = \frac{4\pi^2 \eta_{\text{toluene}}^2 \left( \frac{dn}{dc} \right)^2}{N_A \lambda^4} \text{ (equation S6) and } q = \frac{4\pi \eta_{\text{solvent}} \sin\left(\frac{\theta}{2}\right)}{\lambda} \text{ (equation S7)}$$

With  $\eta$ ,  $\frac{dn}{dc}$ ,  $N_A$ ,  $\lambda$ ,  $\theta$  being the refractive index, refractive index increment, Avogadro constant, wavelength of incident light and the scattering angle. Since all copolymers consist for the most part out of a poly(ethylene glycol) analogue (Jeffamine M-1000), we used the  $dn/dc$  reported for poly(ethylene glycol) for the calculation of the  $M_w$ .<sup>S3</sup> Because of the angle-independence ( $q(\theta) \approx q(0)$ ), and the assumption that interparticle interactions are negligible, the Y-intercept in a plot of  $\frac{R_\theta}{Kc}$  versus  $q^2$  corresponds to the polymer's weight-average molecular mass.

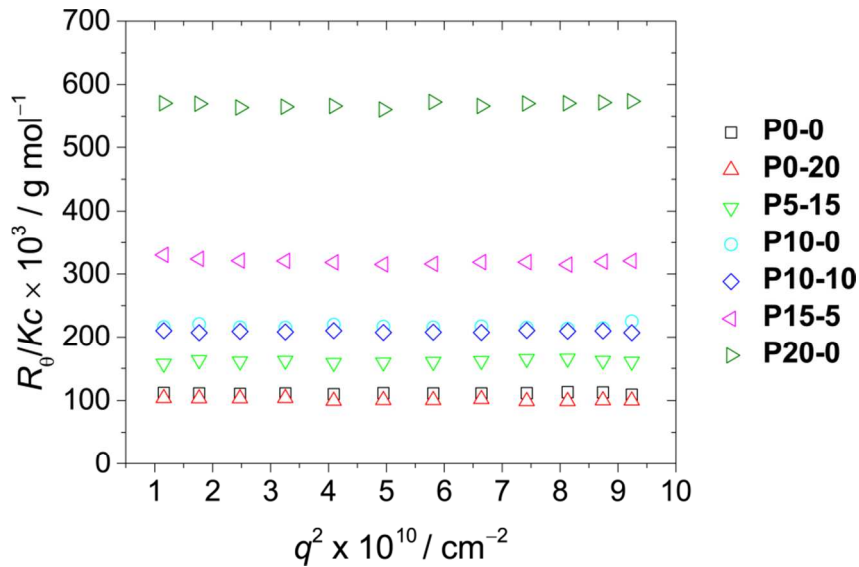


**Figure S28:** The approximate weight-average molecular weight of the nanoparticles formed by the copolymers in solution, determined via SLS ( $c_{\text{polymer}} = 1 \text{ mg mL}^{-1}$ ,  $T = 20 \text{ }^\circ\text{C}$ ,  $dn/dc = 0.135 \text{ mL g}^{-1}$ ).<sup>S3</sup>

## 6. Circular dichroism spectroscopy

Measurements were performed on a Jasco J-815 circular dichroism (CD) spectropolarimeter equipped with a PFD-425S/15 Peltier-type temperature controller. Samples were diluted to a BTA grafts concentration ( $c_{\text{BTA}}$ ) of  $5 \times 10^{-5} \text{ mol L}^{-1}$ , filtered using poly(vinylidene difluoride) (PVDF) syringe filters with pores of  $0.2 \mu\text{m}$ , and measured in a cuvette of quartz with an optical path length of 5 mm. The molar circular dichroism  $\Delta\epsilon$  was calculated using  $\Delta\epsilon = \text{CD effect} / (32980 \times c_{\text{BTA}} \times l)$ , in which  $c$  is the concentration of the BTAs attached to the polymer and  $l$  is the optical pathway. The temperature-dependent CD measurements were performed by monitoring the magnitude of the CD effect ( $\Delta\epsilon$ ) at a single wavelength ( $\lambda = 230 \text{ nm}$ ) during heating and cooling. A cooling rate of  $60 \text{ }^\circ\text{C hr}^{-1}$  was used over the required temperature regime.

**Table S2:** Overview of the polymer concentrations ( $c_{\text{BTA}} = 5 \times 10^{-5} \text{ mol L}^{-1}$ ) in the circular dichroism spectroscopy measurements.

	$c_{\text{polymer}}$ $\text{mg mL}^{-1}$
<b>P0-0</b>	-
<b>P0-20</b>	-
<b>P5-15</b>	0.95
<b>P10-0</b>	0.53
<b>P10-10</b>	0.49
<b>P15-5</b>	0.33
<b>P20-0</b>	0.26

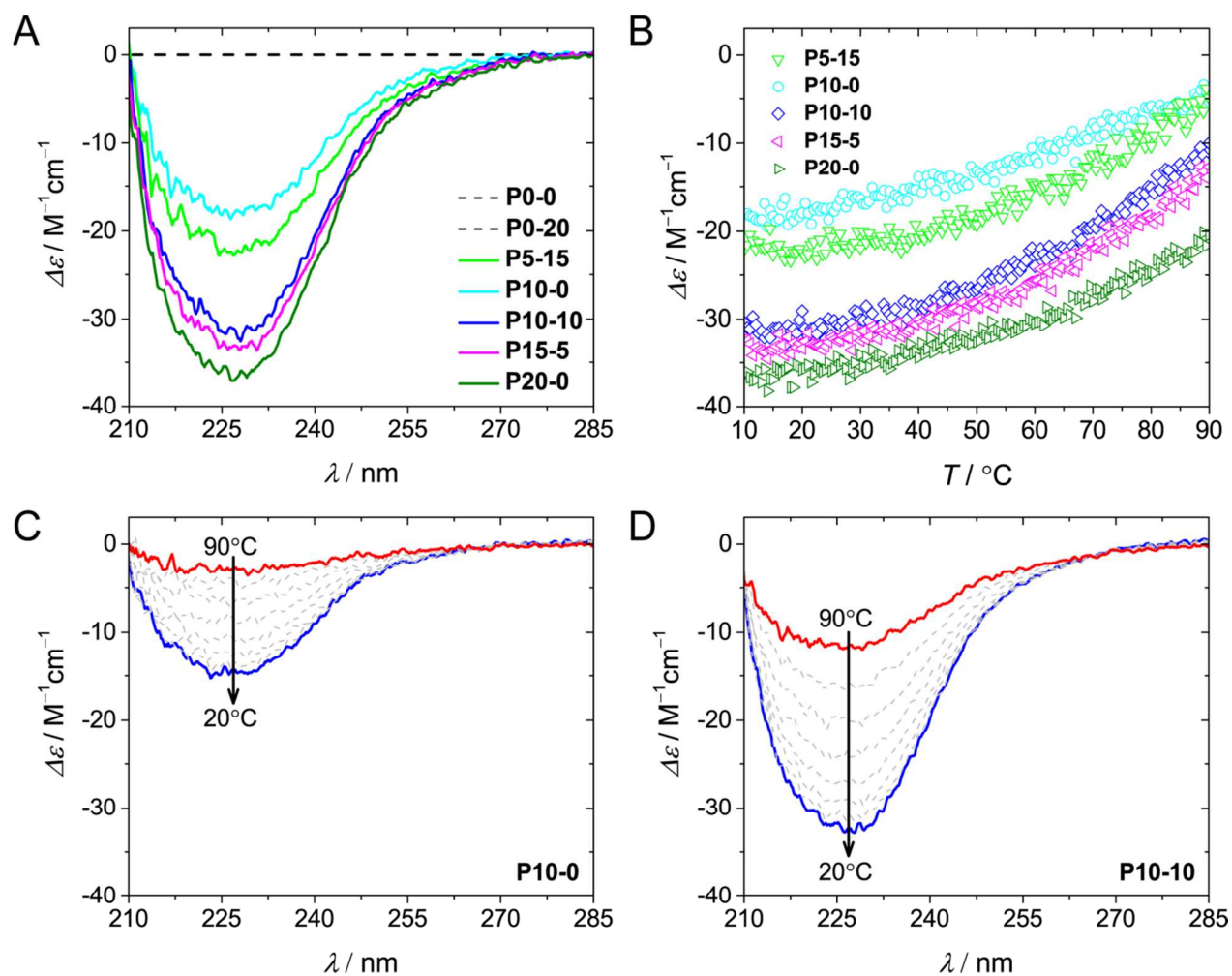


**Figure S29:** A) Comparison of the CD spectra obtained for the BTA-containing polymers ( $c_{\text{BTA}} = 50 \mu\text{M}$ ,  $T = 20^\circ\text{C}$ ), B) The heating curves of the BTA-containing polymers ( $c_{\text{BTA}} = 50 \mu\text{M}$ ,  $\lambda = 230 \text{ nm}$ ), C) The CD spectra of **P10-0** as a function of temperature ( $c_{\text{BTA}} = 50 \mu\text{M}$ ), D) The CD spectra of **P10-10** as a function of temperature ( $c_{\text{BTA}} = 50 \mu\text{M}$ ).

## 7. Small-angle neutron scattering

Small-angle neutron scattering (SANS) experiments were performed at the Larmor instrument of ISIS at the STFC Rutherford Appleton Laboratory. The observed  $q$ -range was  $0.004 \text{ \AA}^{-1} < q < 0.8 \text{ \AA}^{-1}$ , where  $q$  is the magnitude of the scattering vector  $q = \frac{4\pi}{\lambda} \cdot \sin\left(\frac{\theta}{2}\right)$ , with  $\lambda$  being the neutron wavelength and  $\theta$  the scattering angle. The 2D images were radially averaged to obtain the intensity  $I(q)$  vs  $q$  profiles and calibrated to absolute scale using MilliQ water as reference. Standard data reduction procedures, i.e. subtraction of the empty capillary and solvent contribution, were applied by making use of the MantidPlot software.

### Radii of gyration and $I_0$

The radii of gyration and  $I_0$ 's were determined via the shape-independent Guinier analysis. The fitting range was determined such that the maximum  $q$  to be included is  $1.3/R_g$  or less. Furthermore, the first four points were systematically excluded from the fits, since concentration-dependent measurements suggested them to be error-prone. The Guinier analysis was not performed for **P20-0**, because its scattering curve did not reach a plateau.

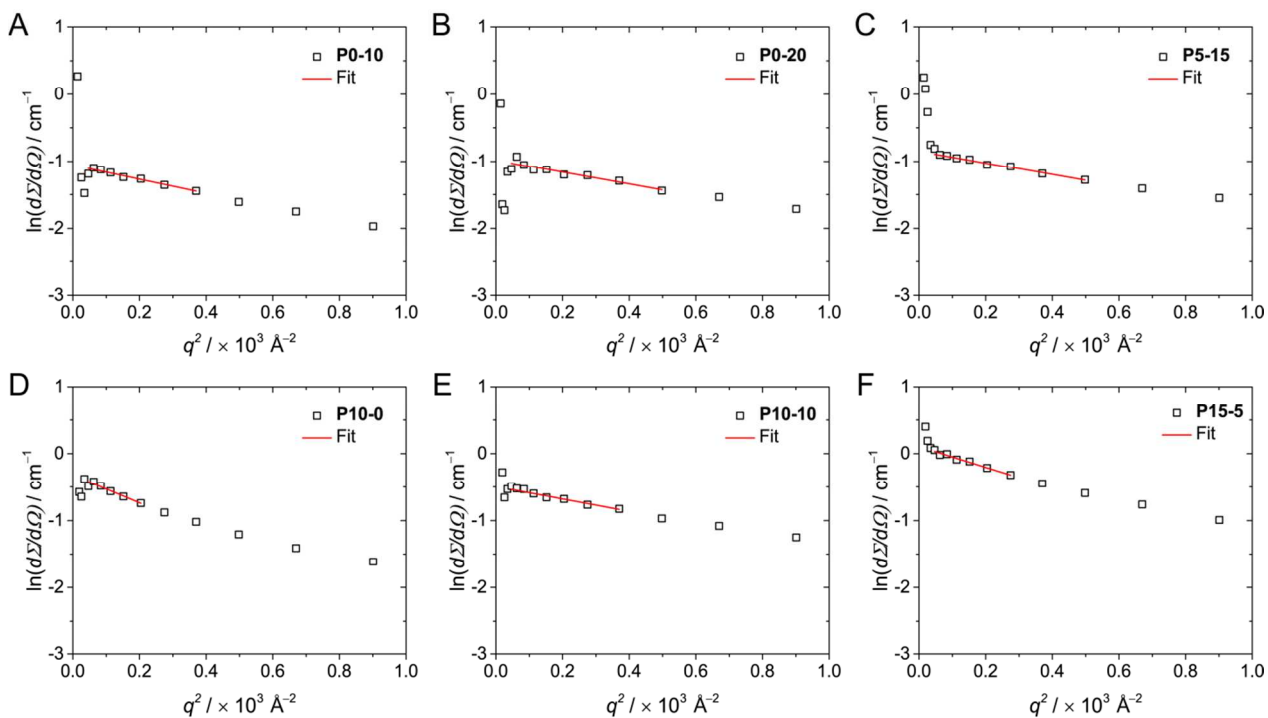


**Figure S30:** The Guinier analysis to determine the polymer's  $R_G$  ( $c_{\text{polymer}} = 1 \text{ mg mL}^{-1}$ ,  $25 \text{ }^\circ\text{C}$ ). A) **P0-0**, B) **P0-20**, C) **P5-15**, D) **P10-0**, E) **P10-10**, F) **P15-5**.

## Molecular weights

The absolute intensity of the scattering profiles was used to calculate the molecular weights of the particles in solution, using:

$$M_{w, SANS} = I_0 \frac{N_A}{c \cdot \Delta\rho_M^2} \text{ (equation S8)}$$

With  $M_{SANS}$  as the molecular weight, the absolute forward scattered intensity ( $I_0$ ), Avogadro constant ( $N_A$ ), polymer concentration ( $c$ ) and the scattering length density difference per mass ( $\Delta\rho_M$ ). This  $\Delta\rho_M$  was calculated according to:

$$\Delta\rho_M = \Delta\rho \cdot \overline{v}_{app} \text{ (equation S9)}$$

Where  $\Delta\rho$  is the scattering length density difference and  $\overline{v}$  is the apparent specific volume of the particles in solution. The scattering length densities for the different polymers were calculated using the SASview software package assuming a density of 1.12 g mL<sup>-3</sup>, corresponding to the density of Jeffamine M-1000. The apparent specific volume of the polymer in solution was determined via:

$$\overline{v}_{app} = \frac{\left(1 - \frac{\Delta d}{c}\right)}{d_{solvent}} \text{ (equation S10)}$$

Containing the density difference between the polymer solution and pure solvent ( $\Delta d$ ), the density of the pure solvent ( $d_{solvent}$ ) and the polymer concentration ( $c$ ). The densities were determined for polymer concentration of 4, 3, 2, 1 and 0 mg mL<sup>-1</sup>.

Aggregation numbers were determined using:

$$N_{agg} = \frac{M_{w, SANS}}{M_{w, Calc.}} \text{ (equation S11)}$$

$M_{w, Calc.}$  was calculated via the following formula:

$$M_{w, Calc. (P_{x-y})} = \left[ (M_{BTA} \times \text{mol}\%_{BTA}) + (M_{Dodecyl} \times \text{mol}\%_{Dodecyl}) + (M_{Jeffamine M-1000} \times \text{mol}\%_{Jeffamine M-1000}) + M_{endgroups} \right] \times D_{M, (P_{x-y})} \text{ (equation S12)}$$

For example:

$$\begin{aligned} M_{w, Calc. (P5-15)} &= [(711.11 \times 5) + (239.42 \times 15) + (1096.37 \times 80) + 194.25] \times 1.24 \\ &= 117.9 \text{ kDa} \end{aligned}$$

**Table S3:** Molecular weights ( $M_{\text{SANS}}$ ) and aggregation numbers ( $N_{\text{agg}}$ ) as determined from the scattered intensity for  $q \rightarrow 0 \text{ nm}^{-1}$ .

Polymer	$\rho_{\text{Polymer}}^a$ ( $\cdot 10^9 \text{ cm}^{-2}$ )	$\rho_{\text{Solvent}}^a$ ( $\cdot 10^{10} \text{ cm}^{-2}$ )	$\Delta\rho^b$ ( $\cdot 10^{10} \text{ cm}^{-2}$ )	$d_{\text{Polymer}}^c$ ( $\text{cm}^{-3} \text{ g}$ )	$d_{\text{Solvent}}^c$ ( $\text{cm}^{-3} \text{ g}$ )	$c_{\text{polymer}}$ ( $\text{g cm}^{-3}$ )	$\overline{v_{\text{app}}}^d$ ( $\text{cm}^3 \text{ g}^{-1}$ )	$\Delta\rho_{\text{M}}^e$ ( $\cdot 10^{10} \text{ cm g}^{-1}$ )	$I_0^f$ ( $\text{cm}^{-1}$ )	$M_{\text{w, SANS}}^g$ (kDa)	$M_{\text{w, calc}}^h$ (kDa)	$N_{\text{agg}}^i$ -
<b>P0-0</b>	6.41	6.40	-5.76	1.10442	1.10451	9.96	0.9826	-5.66	0.346	65.3	127.4	0.51
<b>P0-20</b>	5.41	6.40	-5.86	1.10439	1.10451	9.96	1.0117	-5.93	0.372	64.0	109.4	0.58
<b>P5-15</b>	5.60	6.40	-5.84	1.10445	1.10451	9.97	0.9517	-5.56	0.425	83.1	117.9	0.70
<b>P10-0</b>	6.28	6.40	-5.77	1.10446	1.10451	9.87	0.9467	-5.46	0.609	124.5	127.2	0.98
<b>P10-10</b>	5.78	6.40	-5.82	1.10460	1.10451	9.92	0.8224	-4.79	0.722	191.1	119.8	1.60
<b>P15-5</b>	5.96	6.40	-5.80	1.10438	1.10451	9.97	1.0171	-5.90	1.090	189.0	117.7	1.60
<b>P20-0</b>	6.14	6.40	-5.79	1.10442	1.10451	9.24	0.9847	-5.70	2.200	441.6	120.5	3.66

<sup>a</sup> Calculated using the SASview software package. <sup>b</sup> Calculated via  $\Delta\rho = \rho_{\text{Polymer}} - \rho_{\text{Solvent}}$ . <sup>c</sup> Determined using a densimeter at 20 °C,  $d_{\text{Polymer}}$ . <sup>d</sup> Calculated via  $\overline{v_{\text{app}}} = \left(1 - \frac{\Delta d}{c}\right) / d_{\text{solvent}}$ . <sup>e</sup> Calculated via  $\Delta\rho_{\text{M}} = \Delta\rho \times \overline{v_{\text{app}}}$ . <sup>f</sup> Determined using the Guinier analysis. <sup>g</sup>  $M_{\text{w, SANS}} = I_0 \frac{N_A}{c \cdot \Delta\rho_{\text{M}}^2}$ . <sup>h</sup>  $M_{\text{w, Calc. (P-x-y)}} = [(M_{\text{BTA}} \times \text{mol}\%_{\text{BTA}}) + (M_{\text{Dodecyl}} \times \text{mol}\%_{\text{Dodecyl}}) + (M_{\text{Jeffamine M-1000}} \times \text{mol}\%_{\text{Jeffamine M-1000}}) + M_{\text{endgroups}}] \times D_{\text{M, (P-x-y)}}$ . <sup>i</sup>  $N_{\text{agg}} = M_{\text{w, SANS}} / M_{\text{w, Calc.}}$ .



## 8. References

- S1. Perrier, S.; Takolpuckdee, P.; Mars, C. A. Reversible Addition–Fragmentation Chain Transfer Polymerization: End Group Modification for Functionalized Polymers and Chain Transfer Agent Recovery. *Macromolecules* **2006**, 38, 2033–2036.
- S2. Wu, H. Correlations between the Rayleigh Ratio and the Wavelength for Toluene and Benzene. *Chemical Physics* **2010**, 367, 44-47.
- S3. Michielsen S. In *Polymer Handbook*, 3<sup>rd</sup> ed.; Brandrup, J.; Immergut, E. H.; Grulke E. A., Eds.; John Wiley & Sons, New York, **1999**.